Peralkylated Four- and Five-Membered Cyclosilanes Containing a Heteroatom: Synthesis, Structure, and Properties

Hamao Watanabe,*[a] Hideo Suzuki,[a] Syuji Takahashi,[a] Kiichiro Ohyama,[a] Yuji Sekiguchi,[a] Hideki Ohmori,[a] Michio Nishiyama,[a] Michihiro Sugo,[a] Minoru Yoshikawa,[a] Nobuo Hirai,[a] Yoichi Kanuma,[a] Takahiro Adachi,[a] Masami Makino,[a] Katsura Sakata,[b] Kentaro Kobayashi,[b] Takako Kudo,*[b] Haruo Matsuyama,[c] Nobumasa Kamigata,[c] Michio Kobayashi,[c] Masashi Kijima,*[d] Hideki Shirakawa,[d] Kazumasa Honda,[e] and Midori Goto*[e]

Keywords: HOMO−LUMO interactions / Photolysis / Small ring systems / Silicon / Strained molecules

Seventeen peralkylated four- and five-membered heteroatom-containing silacycles $[R^1R^2Si]_nX$ [R^1 = *i*Pr and/or R^2 = tBuCH$_2$; n = 3; X = CH$_2$ (**1a**, **1b**), NR^3 (R^3 = C_6H_{11}) (**3a**–**d**), O (**5a**–**c**), and n = 4; X = CH$_2$ (**2a**, **2b**), NR^3 (R^3 = C_6H_{11} or Pr) (**4a**–**d**), and O (**6a**, **6b**)] have been synthesized and characterized. The structural features of twelve compounds – **1b**, **3a**–**d**, and **5b** (Si_3X) and **2a**, **4a**–**c**, **6a**, and **6b** (Si_4X) – determined by X-ray analysis have been investigated and geometrical differences between the silacycles bearing neopentyl groups and those with isopropyl groups as bulky substituents on silicon atoms have been identified. The ring strain energies for the compounds $[R_2Si]_nX$ [n = 3, 4; R = Me, *i*Pr; X = CH$_2$, N(*i*Pr), NMe, O, SiH$_2$], estimated by theoretical calculations at the PM3 level, are discussed in relation to experimentally ascertained structural features of the silacycles $[R_2Si]_nX$ (n = 3, 4; R = *i*Pr; X = CH$_2$, NC$_6$H$_{11}$, O, SiR$_2$). ^{29}Si NMR spectra for **1**–**6** showed that the resonances for the α-silicon atoms attached to the heteroatoms X in the two ring-size series were shifted downfield by a deshielding effect due to an electronegative atom X; larger electronegativity (*En*) of X caused this effect at lower field. The chemical shifts of the Si$^{\alpha}$ atoms showed a good linear correlation with the electronegativities of the heteroatoms X in the $[R_2Si]_nX$ cycles. In the UV spectra for **1**–**6**, little difference in the longest-wavelength absorption (LWA) maxima was observed for $[(iPr)_2Si]_nX$ and $[(tBuCH_2)_2Si]_nX$ of the same ring size. The LWA bands for **1**–**6** and related compounds could be roughly classified into four groups: (a) $[R_2Si]_3X$ (X = SiR$_2$, GeR′$_2$) λ = 286–300 nm; (b) $[R_2Si]_3X$ (X = CH$_2$, NR^3, O) (**1**, **3**, **5**), λ = 230–250 nm; (c) $[R_2Si]_4X$ (X = SiR$_2$, GeR′$_2$) λ = 274–280 nm; (d) $[R_2Si]_4X$ (X = CH$_2$, NR^3, O) (**2**, **4**, **6**), λ = 250–260 nm. With the aid of the ionization potentials and the transition energies (E_T), the HOMO and LUMO levels for the series of compounds and the related ones were experimentally evaluated. The HOMO and LUMO levels thus obtained for $[R_2Si]_3X$ and $[R_2Si]_4X$ (R = *i*Pr and tBuCH$_2$; X = SiR$_2$, GeR′$_2$, CH$_2$, NC$_6$H$_{11}$, O) are discussed in terms of the calculated values and frontier orbitals on the basis of PM3 levels. The theoretical prediction for bond scission in the silacycles $[(iPr)_2Si]_nX$ (n = 3, 4; X = CH$_2$, NMe, O) in which the HOMOs and LUMOs have Si–Si bonding and antibonding character, respectively, was corroborated by the good agreement with experimental results from photolysis of the silacycles $[R_2Si]_nX$ (n = 3, 4; R = *i*Pr and tBuCH$_2$; X = CH$_2$, NC$_6$H$_{11}$, O), with bond scission occurring only at the Si–Si bonds, and not at the Si–X bonds.

[a] Department of Materials Science, Faculty of Engineering, Gunma University,
Kiryu, Gunma 376-8515, Japan
Fax: (internat.) + 81-277/47-5453
E-mail: hwatanab@chem.gunma-u.ac.jp
[b] Department of Fundamental Studies, Faculty of Engineering, Gunma University,
Kiryu, Gunma 376-8515, Japan
[c] Department of Chemistry, Faculty of Science, Tokyo Metropolitan University,
Hachioji, Tokyo, 192-0397, Japan
[d] Institute of Materials Science, University of Tsukuba,
Tsukuba, Ibaraki, 305-8571, Japan
[e] National Institute of Materials and Chemical Research,
Tsukuba, Ibaraki, 305-8565, Japan
Supporting information for this article is available on the WWW under http://www.eurjic.com or from the author.

Introduction

The chemistry of silacycles containing a heteroatom such as oxygen, nitrogen, etc. comprises an intriguing subject worthy of study regarding their properties. Although a large number of studies of homosilacycles Si_n,[1] and of heteroatom-containing silacycles such as Si_nGe,[2] Si_nC,[3] Si_nN,[4] and Si_nO[5] have appeared, there are only limited systematic studies focusing on the series of heteroatom-containing silacycles Si_nX from the perspective of properties arising from the presence of X as a heteroatom.[6] We have previously studied some properties of various peralkylated cyclosilanes $[R^1R^2Si]_n$ (n = 3−7)[7] and have also reported

preliminary results for $[R_2Si]_3O$.[8] Recently, we described the synthesis, molecular structure, and photolysis of the $[R_2Si]_nGeR'_2$ series [n = 2: R = tBuCH$_2$, R′ = Me$_3$SiCH$_2$;[9] n = 3: R = iPr, tBuCH$_2$, R′ = Me$_3$SiCH$_2$ (**C**, **D**);[10] and n = 4: R = iPr, tBuCH$_2$, R′ = Me$_3$SiCH$_2$, Ph (**G**–**I**)[11]].

This paper deals with a full account of the series of heteroatom-containing four- and five-membered cyclosilanes $[R^1R^2Si]_nX$ [n = 3, 4; R^1, R^2 = iPr, tBuCH$_2$; X = CH$_2$ (**1**, **2**), NR^3 (R^3 = C$_6$H$_{11}$ or Pr) (**3**, **4**), O (**5**, **6**)], as shown in Scheme 1, including molecular structures determined by X-ray crystal analysis, some properties such as ^{29}Si NMR and UV spectra, and oxidation and ionization potentials. We have performed semiempirical PM3[12] molecular orbital calculations for a series of heterosubstituted silacycles $[R_2Si]_nX$ [n = 3, 4; R = Me, iPr; X = SiH$_2$, CH$_2$, NMe, N(iPr), O] in order to estimate the ring strain energies. The energy levels and character of their frontier orbitals are also discussed in relation to their molecular structures, oxidation and ionization potentials, and photochemical reactions of the series of heterosilacycles obtained experimentally in the current study.

Results and Discussion

Synthesis

Compounds **1** and **2** were synthesized in good yields (72–92%) by reductive coupling of the corresponding α,ω-dichlorocarbosilanes with lithium in THF at room temperature [Scheme 2, (a)]. Compounds **3** and **4** were synthesized in moderate yields (35–69%) by treatment of the corresponding α,ω-dichlorosilanes with lithium alkylamides [Scheme 2, (b) and (c)]. Compounds **5** and **6** were synthesized by hydrolytic cyclization with the corresponding α,ω-dichlorosilanes, in good yields (88–96%) except in the case of **5a** (28%) [Scheme 2, (d)]. Compound **E** was also prepared from the corresponding 1,4-dilithiotetrasilane and dichlorosilane in a reasonable yield [Scheme 2, (e)]. All the compounds **1**–**6** obtained were found to be air- and moisture-stable liquids (**1a**, **5c**) or crystals (the others) and were identified in the usual manner (NMR, IR, and MS data, as well as elemental analysis), while $[Me_2Si]_3CH_2$[3a] and $[Ph_2Si]_4X$ (X = NMe, NEt, O)[6e] have been reported to be air- and moisture-sensitive compounds.

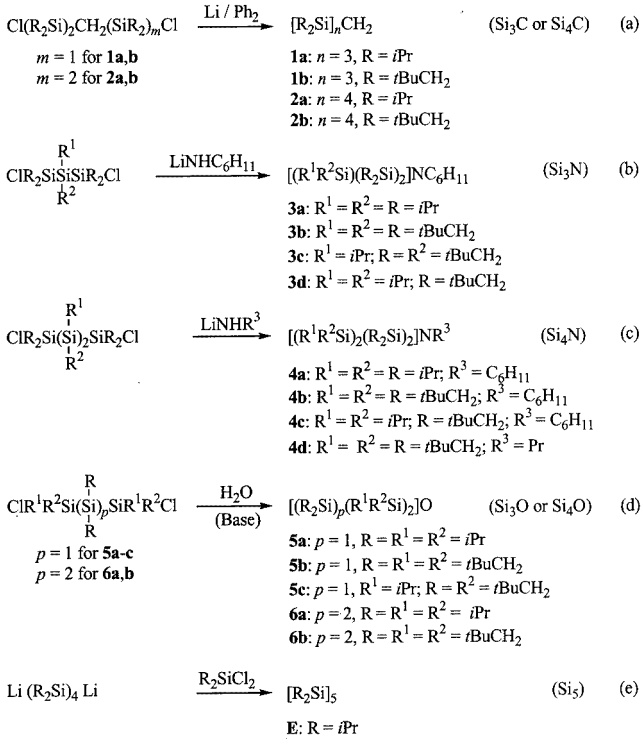

Scheme 2. (a–e) Synthetic methods for heteroatom-containing silacycles Si_nX [n = 3, 4; X = CH$_2$, NR^3 and O; n = 4, X = Si(iPr)$_2$]

Molecular Structures

Except for Si_3C[3a] and Si_4O,[5g] there are no precedents for structural studies on the ring systems Si_4C, Si_nN (n = 3, 4), and Si_nO (n = 3, 4). The molecular structures of **1b**,

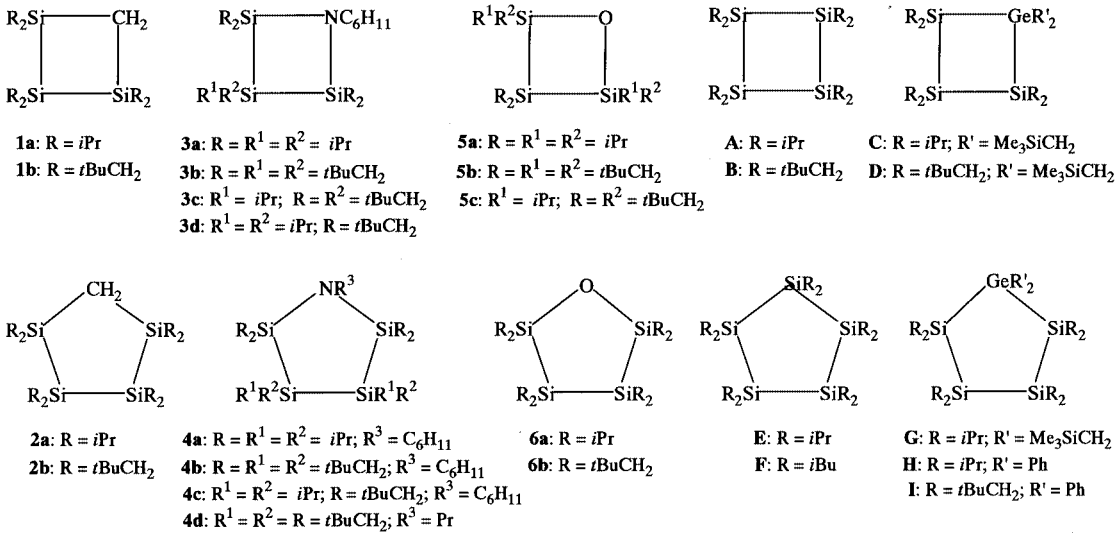

Scheme 1. Molecular formula of heteroatom-containing silacycles and related compounds

2a, **3a–d**, **4a–c**, **5b**, **6a**, and **6b** were determined by X-ray crystal analysis; structural data for **1a** and **5a** could not be obtained by X-ray analysis. Selected bond lengths and bond and torsion angles for these compounds are listed in Tables 1–12, and the pertinent geometrical data needed for structural discussion of $[R_2Si]_3X$ and $[R_2Si]_4X$ (X = C, N O) and the related compounds **A–E**, **H**, and **I** are summarized in Tables 13 and 14.

(1) Bond Lengths and Angles

The Si_3C ring of **1b** was found to be moderately puckered, with a dihedral angle of 25.5°, and the Si_4C ring of **2a** to be a slightly deformed envelope conformation. The structural data for four known Si_3C ring compounds[3b–3d]

Table 1. Selected bond lengths [Å], bond angles [°], and torsion angles [°] in **1b**

Bond distances					
Si(1)-Si(2)	2.400(2)	Si(2)-Si(3)	2.387(4)	Si(1)-C(1)	1.882(5)
Si(3)-C(1)	1.895(6)	Si(1)-C(2)	1.882(7)	Si(1)-C(7)	1.905(6)
Si(2)-C(12)	1.906(6)	Si(2)-C(17)	1.914(6))	Si(3)-C(22)	1.890(6)
Si(3)-C(27)	1.900(6)				
Bond angles					
Si(1)-Si(2)-Si(3)	75.9(1)	Si(2)-Si(3)-C(1)	88.0(2)		
Si(2)-Si(1)-C(1)	87.9(2)	Si(1)-C(1)-Si(3)	102.3(3)		
C(2)-Si(1)-C(7)	113.0(3)	C(12)-Si(2)-C(17)	115.4(3)		
C(22)-Si(3)-C(27)	115.8(3)				
Torsion angles					
Si(1)-Si(2)-Si(3)-C(1)	-16.2(1)	Si(2)-Si(3)-C(1)-Si(1)	20.7(2)		
Si(3)-C(1)-Si(1)-Si(2)	-20.6(2)	C(1)-Si(1)-Si(2)-Si(3)	16.3(1)		

Table 2. Selected bond lengths [Å], bond angles [°], and torsion angles [°] in **2a**

Bond distances					
Si(1)-Si(2)	2.384(2)	Si(2)-Si(3)	2.391(2)	Si(3)-Si(4)	2.403(2)
Si(1)-C(1)	1.896(4)	Si(4)-C(1)	1.877(5)	Si(1)-C(2)	1.880(6)
Si(1)-C(5)	1.906(6)	Si(2)-C(8)	1.917(5)	Si(2)-C(11)	1.910(6)
Si(3)-C(14)	1.921(5)	Si(3)-C(17)	1.906(6)	Si(4)-C(20)	1.891(5)
Si(4)-C(23)	1.940(7)				
Bond angles					
Si(1)-Si(2)-Si(3)	96.9(1)	Si(2)-Si(3)-Si(4)	98.0(1)		
Si(3)-Si(4)-C(1)	105.4(1)	Si(2)-Si(1)-C(1)	99.9(1)		
Si(1)-C(1)-Si(4)	117.7(2)	C(2)-Si(1)-C(5)	113.9(3)		
C(8)-Si(2)-C(11)	110.4(3)	C(14)-Si(3)-C(17)	109.8(3)		
C(20)-Si(4)-C(23)	114.4(3)				
Torsion angles					
Si(1)-Si(2)-Si(3)-Si(4)	-28.5(1)	Si(2)-Si(3)-Si(4)-C(1)	7.3(2)		
Si(3)-Si(4)-C(1)-Si(1)	26.4(3)	Si(4)-C(1)-Si(1)-Si(2)	-47.1(3)		
C(1)-Si(1)-Si(2)-Si(3)	43.6(2)				

Table 3. Selected bond lengths [Å], bond angles [°], and torsion angles [°] in **3a**

Bond distances					
Si(1)-Si(2)	2.362(2)	Si(1)-Si(3)	2.377(2)	Si(2)-N(1)	1.757(4)
Si(3)-N(1)	1.757(4)	Si(2)-C(21)	1.898(6)	Si(2)-C(22)	1.903(7)
Si(1)-C(11)	1.904(6)	Si(1)-C(12)	1.907(6))	Si(3)-C(31)	1.901(5)
Si(3)-C(32)	1.919(6)	N(1)-C(41)	1.485(7)		
Bond angles					
Si(2)-Si(1)-Si(3)	74.5(1)	Si(1)-Si(2)-N(1)	88.2(1)		
Si(1)-Si(3)-N(1)	87.7(1)	Si(2)-N(1)-Si(3)	109.5(2)		
C(21)-Si(2)-C(22)	108.2(3)	C(11)-Si(1)-C(12)	112.0(3)		
C(31)-Si(3)-C(32)	103.9(2)	Si(2)-N(1)-C(41)	120.3(3)		
Si(3)-N(1)-C(41)	130.1(3)				
Torsion angles					
Si(3)-Si(1)-Si(2)-N(1)	2.1(1)	Si(2)-Si(1)-Si(3)-N(1)	-2.1(1)		
Si(1)-Si(2)-N(1)-Si(3)	-2.9(2)	Si(1)-Si(3)-N(1)-Si(2)	2.9(2)		

Table 4. Selected bond lengths [Å], bond angles [°], and torsion angles [°] in **3b**

Bond distances					
Si(1)-Si(2)	2.365(2)	Si(2)-Si(3)	2.395(2)	Si(1)-N(1)	1.758(3)
Si(3)-N(1)	1.768(3)	Si(1)-C(27)	1.907(4)	Si(1)-C(32)	1.899(5)
Si(2)-C(17)	1.908(5)	Si(2)-C(22)	1.917(6)	Si(3)-C(7)	1.906(6)
Si(3)-C(12)	1.903(7)	N(1)-C(1)	1.485(4)		
Bond angles					
Si(1)-Si(2)-Si(3)	74.3(1)	Si(2)-Si(3)-N(1)	85.8(1)		
Si(2)-Si(1)-N(1)	86.9(1)	Si(1)-N(1)-Si(3)	109.3(2)		
C(27)-Si(2)-C(32)	113.0(2)	C(17)-Si(2)-C(22)	114.0(2)		
C(7)-Si(3)-C(12)	111.0(3)	Si(1)-N(1)-C(1)	121.7(2)		
Si(3)-N(1)-C(1)	129.0(3)				
Torsion angles					
Si(1)-Si(2)-Si(3)-N(1)	-12.2(1)	Si(2)-Si(3)-N(1)-Si(1)	16.9(1)		
Si(3)-N(1)-Si(1)-Si(2)	-17.1(2)	N(1)-Si(1)-Si(2)-Si(3)	12.3(1)		

Table 5. Selected bond lengths [Å], bond angles [°], and torsion angles [°] in **3c**

Bond distances					
Si(1)-Si(2)	2.373(1)	Si(2)-Si(3)	2.394(1)	Si(1)-N(1)	1.755(2)
Si(3)-N(1)	1.770(2)	Si(1)-C(1)	1.909(3)	Si(1)-C(6)	1.902(3)
Si(2)-C(11)	1.911(3)	Si(2)-C(16)	1.927(4)	Si(3)-C(19)	1.907(4)
Si(3)-C(24)	1.907(3)	N(1)-C(29)	1.484(3)		
Bond angles					
Si(1)-Si(2)-Si(3)	74.0(1)	Si(2)-Si(3)-N(1)	85.4(1)		
Si(2)-Si(1)-N(1)	86.4(1)	Si(1)-N(1)-Si(3)	108.9(1)		
C(11)-Si(2)-C(16)	109.0(1)	C(1)-Si(1)-C(16)	111.6(1)		
C(19)-Si(3)-C(24)	108.3(1)	Si(1)-N(1)-C(29)	122.0(1)		
Si(3)-N(1)-C(29)	128.9(1)				
Torsion angles					
Si(1)-Si(2)-Si(3)-N(1)	-14.6(8)	Si(2)-Si(1)-N(1)-Si(3)	-20.4(1)		
Si(1)-N(1)-Si(3)-Si(2)	20.2(1)	Si(3)-Si(2)-Si(1)-N(1)	-14.7(9)		

Table 6. Selected bond lengths [Å], bond angles [°], and torsion angles [°] in **3d**

Bond distances					
Si(1)-Si(2)	2.399(3)	Si(2)-Si(3)	2.360(3)	Si(1)-N(1)	1.778(5)
Si(3)-N(1)	1.757(5)	Si(1)-C(7)	1.912(8)	Si(1)-C(12)	1.901(9)
Si(2)-C(17)	1.900(8)	Si(2)-C(20)	1.921(8)	Si(3)-C(23)	1.902(7)
Si(3)-C(28)	1.907(7)	N(1)-C(1)	1.487(8)		
Bond angles					
Si(1)-Si(2)-Si(3)	74.3(1)	Si(2)-Si(3)-N(1)	87.3(2)		
Si(3)-N(1)-Si(1)	108.7(3)	N(1)-Si(1)-Si(2)	85.6(2)		
C(7)-Si(1)-C(12)	105.6(4)	C(17)-Si(2)-C(20)	111.6(4)		
C(23)-Si(3)-C(28)	112.3(3)	Si(1)-N(1)-C(1)	128.8(4)		
Si(3)-N(1)-C(1)	122.5(4)				
Torsion angles					
Si(1)-Si(2)-Si(3)-N(1)	13.2(2)	Si(3)-Si(2)-Si(1)-N(1)	-12.9(2)		
Si(2)-Si(1)-N(1)-Si(3)	17.8(2)	Si(1)-N(1)-Si(3)-Si(2)	-18.0(2)		

Table 7. Selected bond lengths [Å], bond angles [°], and torsion angles [°] in **4a**

Bond distances					
Si(1)-Si(2)	2.410(2)	Si(2)-Si(3)	2.402(3)	Si(3)-Si(4)	2.393(4)
Si(1)-N(1)	1.766(6)	Si(4)N(1)	1.753(6)	Si(1)-C(7)	1.939(7)
Si(1)-C(10)	1.906(7)	Si(2)-C(13)	1.930(7)	Si(2)-C(16)	1.918(8)
Si(3)-C(19)	1.929(8)	Si(3)-C(22)	1.945(8)	Si(4)-C(25)	1.937(10)
Si(4)-C(28)	1.923(9)	C(1)-N(1)	1.517(10)		
Bond angles					
Si(1)-Si(2)-Si(3)	97.0(1)	Si(2)-Si(3)-Si(4)	95.4(1)		
Si(3)-Si(4)-N(1)	106.9(2)	Si(2)-Si(1)-N(1)	105.2(2)		
Si(1)-N(1)-Si(4)	125.6(3)	C(7)-Si(1)-C(10)	104.9(3)		
C(13)-Si(2)-C(16)	109.5(3)	C(19)-Si(3)-C(22)	110.6(3)		
C(25)-Si(4)-C(28)	106.0(5)	C(1)-N(1)-Si(1)	121.9(4)		
C(1)-N(1)-Si(4)	112.5(5)				
Torsion angles					
Si(1)-Si(2)-Si(3)-Si(4)	27.3(10)	Si(2)-Si(3)-Si(4)-N(1)	-26.9(13)		
Si(3)-Si(4)-N(1)-Si(1)	13.3(20)	Si(4)-N(1)-Si(1)-Si(2)	8.3(20)		
N(1)-Si(1)-Si(2)-Si(3)	-24.7(13)				

Table 8. Selected bond lengths [Å], bond angles [°], and torsion angles [°] in **4b**

Bond distances					
Si(1)-Si(2)	2.408(3)	Si(2)-Si(3)	2.377(3)	Si(3)-Si(4)	2.405(3)
Si(1)-N(1)	1.763(7)	Si(4)-N(1)	1.787(6)	Si(1)-C(7)	1.910(12)
Si(1)-C(12)	1.912(10)	Si(2)-C(17)	1.932(13)	Si(2)-C(22)	1.908(15)
Si(3)-C(27)	1.947(11)	Si(3)-C(32)	1.925(10)	Si(4)-C(37)	1.894(14)
Si(4)-C(42)	1.891(14)	C(1)-N(1)	1.518(11)		
Bond angles					
Si(1)-Si(2)-Si(3)	94.4(1)	Si(2)-Si(3)-Si(4)	93.6(1)		
Si(3)-Si(4)-N(1)	105.8(2)	Si(2)-Si(1)-N(1)	101.6(2)		
Si(1)-N(1)-Si(4)	123.2(4)	C(7)-Si(1)-C(12)	109.8(5)		
C(17)-Si(2)-C(22)	117.3(12)	C(27)-Si(3)-C(32)	117.4(5)		
C(37)-Si(4)-C(42)	113.5(6)	C(1)-N(1)-Si(1)	126.0(5)		
C(1)-N(1)-Si(4)	110.8(5)				
Torsion angles					
Si(1)-Si(2)-Si(3)-Si(4)	37.7(1)	Si(2)-Si(3)-Si(4)-N(1)	-27.8(2)		
Si(3)-Si(4)-N(1)-Si(1)	-2.0(5)	Si(4)-N(1)-Si(1)-Si(2)	30.9(4)		
N(1)-Si(1)-Si(2)-Si(3)	-43.5(2)				

Table 9. Selected bond lengths [Å], bond angles [°], and torsion angles [°] in **4c**

Bond distances					
Si(1)-Si(2)	2.408(3)	Si(2)-Si(3)	2.372(2)	Si(3)-Si(4)	2.395(2)
Si(1)-N(1)	1.775(4)	Si(4)-N(1)	1.758(3)	Si(1)-C(7)	1.900(7)
Si(1)-C(12)	1.912(5)	Si(2)-C(17)	1.908(6)	Si(2)-C(20)	1.935(6)
Si(3)-C(23)	1.894(12)	Si(3)-C(26)	1.939(9)	Si(4)-C(29)	1.900(6)
Si(4)-C(34)	1.936(6)	C(1)-N(1)	1.522(6)		
Bond angles					
Si(1)-Si(2)-Si(3)	94.3(1)	Si(2)-Si(3)-Si(4)	94.4(1)		
Si(3)-Si(4)-N(1)	103.4(1)	Si(4)-N(1)-Si(1)	124.4(2)		
N(1)-Si(1)-Si(2)	104.7(1)	C(7)-Si(1)-C(12)	112.3(3)		
C(17)-Si(2)-C(20)	110.3(3)	C(23)-Si(3)-C(26)	113.3(4)		
C(29)-Si(4)-C(34)	111.3(3)	Si(1)-N(1)-C(1)	110.0(3)		
Si(4)-N(1)-C(1)	125.4(3)				
Torsion angles					
Si(1)-Si(2)-Si(3)-Si(4)	-36.9(1)	Si(3)-Si(2)-Si(1)-N(1)	30.8(2)		
Si(2)-Si(1)-N(1)-Si(4)	-5.8(3)	Si(2)-Si(3)-Si(4)-N(1)	38.9(1)		
Si(3)-Si(4)-N(1)-Si(1)	-22.8(3)				

Table 10. Selected bond lengths [Å], bond angles [°], and torsion angles [°] in **5b**

Bond distances					
Si(1)-Si(2)	2.445(5)	Si(2)-Si(3)	2.421(5)	Si(1)-O(1)	1.646(11)
Si(3)-O(1)	1.665(12)	Si(1)-C(1)	1.893(16)	Si(1)-C(2)	1.888(16)
Si(2)-C(3)	1.882(14)	Si(2)-C(4)	1.907(13)	Si(3)-C(5)	1.862(13)
Si(3)-C(6)	1.862(13)				
Bond angles					
Si(1)-Si(2)-Si(3)	68.2(2)	Si(2)-Si(3)-O(1)	90.5(4)		
Si(2)-Si(1)-O(1)	90.1(4)	Si(1)-O(1)-Si(3)	111.1(5)		
C(1)-Si(1)-C(2)	115.5(8)	C(3)-Si(2)-C(4)	117.3(5)		
C(5)-Si(3)-C(6)	115.0(7)				
Torsion angles					
Si(1)-Si(2)-Si(3)-O(1)	-1.7(4)	Si(1)-O(1)-Si(3)-Si(2)	2.6(6)		
Si(2)-Si(1)-O(1)-Si(3)	-2.5(6)	Si(3)-Si(2)-Si(1)-O(1)	1.7(4)		

Table 11. Selected bond lengths [Å], bond angles [°], and torsion angles [°] in **6a**

Bond distances					
Si(1)-Si(2)	2.402(2)	Si(2)-Si(3)	2.389(2)	Si(3)-Si(4)	2.386(2)
Si(1)-O(1)	1.638(3)	Si(4)-O(1)	1.654(3)	Si(1)-C(1)	1.901(6)
Si(1)-C(4)	1.887(5)	Si(2)-C(7)	1.917(5)	Si(2)-C(10)	1.901(6)
Si(3)-C(13)	1.900(5)	Si(3)-C(16)	1.892(6)	Si(4)-C(19)	1.896(6)
Si(4)-C(22)	1.880(7)				
Bond angles					
Si(1)-Si(2)-Si(3)	95.4(1)	Si(2)-Si(3)-Si(4)	95.2(1)		
Si(3)-Si(4)-O(1)	100.8(1)	Si(2)-Si(1)-O(1)	103.1(1)		
Si(1)-O(1)-Si(4)	133.6(2)	C(1)-Si(1)-C(4)	114.2(2)		
C(7)-Si(2)-C(10)	109.5(3)	C(13)-Si(3)-C(16)	109.8(3)		
C(19)-Si(4)-C(22)	115.0(3)				
Torsion angles					
Si(1)-Si(2)-Si(3)-Si(4)	-25.9(1)	Si(2)-Si(3)-Si(4)-O(1)	32.1(1)		
Si(3)-Si(4)-O(1)-Si(1)	-30.5(3)	Si(4)-O(1)-Si(1)-Si(2)	9.8(3)		
O(1)-Si(1)-Si(2)-Si(3)	16.5(1)				

Table 12. Selected bond lengths [Å], bond angles [°], and torsion angles [°] in **6b** (molecule A and molecule B)

molecule A					
Bond distances					
Si(1)-Si(2)	2.450(4)	Si(2)-Si(3)	2.413(4)	Si(3)-Si(4)	2.404(4)
Si(1)-O(1)	1.610(8)	Si(4)-O(1)	1.667(8)	Si(1)-C(1)	1.93(1)
Si(1)-C(6)	1.89(1)	Si(2)-C(11)	1.89(1)	Si(2)-C(16)	1.90(1)
Si(3)-C(21)	1.89(1)	Si(3)-C(26)	1.91(1)	Si(4)-C(31)	1.91(1)
Si(4)-C(36)	1.91(1)				
Bond angles					
Si(1)-Si(2)-Si(3)	92.0(1)	Si(2)-Si(3)-Si(4)	93.8(1)		
Si(3)-Si(4)-O(1)	102.4(3)	Si(2)-Si(1)-O(1)	103.4(3)		
Si(1)-O(1)-Si(4)	132.5(4)	C(1)-Si(1)-C(6)	111.3(5)		
C(11)-Si(2)-C(16)	112.4(5)	C(21)-Si(3)-C(26)	112.4(4)		
C(31)-Si(4)-C(36)	109.6(6)				
Torsion angles					
Si(1)-Si(2)-Si(3)-Si(4)	33.3(2)	Si(2)-Si(3)-Si(4)-O(1)	-33.1(3)		
Si(3)-Si(4)-O(1)-Si(1)	15.1(6)	Si(4)-O(1)-Si(1)-Si(2)	12.2(7)		
O(1)-Si(1)-Si(2)-Si(3)	-31.5(3)				
molecule B					
Bond distances					
Si(5)-Si(6)	2.414(4)	Si(6)-Si(7)	2.419(4)	Si(7)-Si(8)	2.383(4)
Si(5)-O(2)	1.583(10)	Si(8)-O(2)	1.664(10)	Si(5)-C(41)	1.94(1)
Si(5)-C(46)	1.91(2)	Si(6)-C(51)	1.89(1)	Si(6)-C(56)	1.91(1)
Si(7)-C(61)	1.94(1)	Si(7)-C(66)	1.94(1)	Si(8)-C(71)	1.91(1)
Si(8)-C(76)	1.90(1)				
Bond angles					
Si(5)-Si(6)-Si(7)	92.2(2)	Si(6)-Si(7)-Si(8)	93.6(1)		
Si(6)-Si(5)-O(2)	104.9(3)	Si(7)-Si(8)-O(2)	102.6(3)		
Si(5)-O(2)-Si(8)	132.0(5)	C(41)-Si(5)-C(46)	113.5(7)		
C(51)-Si(6)-C(56)	112.8(5)	C(61)-Si(7)-C(66)	115.0(5)		
C(71)-Si(8)-C(76)	113.6(5)				
Torsion angles					
Si(5)-Si(6)-Si(7)-Si(8)	-31.9(1)	Si(6)-Si(7)-Si(8)-O(2)	33.3(3)		
Si(7)-Si(8)-O(2)-Si(5)	-19.0(8)	Si(8)-O(2)-Si(5)-Si(6)	-7.6(8)		
O(2)-Si(5)-Si(6)-Si(7)	28.7(4)				

have been reported previously (dihedral angles: 0−14°, Si−Si−Si: 77.2−82.9°, Si−C−Si: 100.8−107.8°, Si−Si distances: 2.389−2.500 Å, Si−$C_{(ring)}$ distances: 1.936−1.983 Å). If the data listed in Tables 1 and 13 for **1b** are compared with those for the known compounds,[3b−3d][6a] the dihedral angle in **1b** is seen to be the largest, and both the Si−Si−Si angle and Si−$C_{(ring)}$ distance in **1b** are the smallest. The Si−Si bond length (2.394 Å) in **1b** is in the range between the known Si_3C cycles.[3b−3d] Among the four inner angles for the Si_3C ring of **1b**, Si−Si−Si (75.9°) is the smallest and Si−C−Si (102.3°) the largest. A similar trend was also observed for the five inner angles of the Si_4C ring of **2a**. The bond lengths of Si−Si (2.393 Å) and Si−$C_{(ring)}$ (1.888 Å)[13] in the Si_4C of **2a** are within the normal ranges.

The four-membered Si_3N cycles of **3a−d** are planar or puckered structures (dihedral angles 21−23°). The five-membered Si_4N cycles of **4a−c** are in distorted half-chair or envelope conformations. The Si−Si bond lengths in **3a−d** are 2.370−2.384 Å. Compound **3a** has nearly the same distance as in cyclotetrasilane **A** (2.373 Å), while those in compounds **3b−d** (average 2.381 Å) are shorter than those in cyclotetrasilane **B** (2.409) by 0.028 Å. On the other hand, the Si−Si bond lengths (2.397−2.402 Å) in the five-membered compounds **4a−c** are, except for the Si^2−Si^3 bond (2.372 Å) in **4c**, very close to each other. The three distances are longer than those in the corresponding four-membered compounds **3a−d**, but shorter than that (2.422 Å) in the related homosilacycle **E**.[14] The Si−N bond lengths in the two sets Si_3N (**3a−d**, 1.757−1.768 Å) and Si_4N (**4a−c**, 1.760−1.775 Å) are comparable with the typical value of 1.70−1.76 Å,[13] those involving neopentyl groups on the silicons being longer than those with isopro-

Table 13. Geometrical data of four-membered heteroatom-containing silacycles $[R_2Si]_3X$

compd	X	R	bond dist. [Å] Si-Si	Si-X	Si^{α}---$Si^{\alpha'}$ [a]	bond angle [deg.] Si-Si-Si	Si-Si-X	Si-X-Si	dihedral angle [deg.]
1b	CH_2	$tBuCH_2$	2.394	1.889	2.95	75.9	88.0	102.3	25.5
3a	NC_6H_{11}	*i*Pr	2.370	1.757	2.90	74.5	88.0	109.5	0
3b	"	$tBuCH_2$	2.380	1.763	2.73	74.3	86.4	109.3	21
3c	"	$tBuCH_2$ *i*Pr	2.384	1.768	2.86	74.0	85.9	108.9	23
3d	"	$tBuCH_2$ *i*Pr	2.380	1.768	2.86	74.3	86.5	108.7	21
5b	O	$tBuCH_2$	2.433	1.656	2.73	68.2	90.3	111.1	3
A [b]	SiR_2	*i*Pr	2.373	2.373	3.30	87.0	87.0	87.0	37
B [c]	"	$tBuCH_2$	2.409	2.409	3.30	86.7	86.7	86.7	39
C [d]	$Ge(CH_2SiMe_3)_2$	*i*Pr	2.386	2.457	3.38	90.4	88.8	87.1	24
D	"	$tBuCH_2$	2.393	2.444	3.35	88.7	86.8	86.4	36

[a] Non-bonding distances. [b] Ref.[7f]. [c] Ref.[16]. [d] Ref.[10]

Table 14. Geometrical data of five-membered heteroatom-containing silacycles $[R_2Si]_4X$

compd	X	R	bond dist. [Å] Si-Si	Si-X	bond angle [deg.] Si-Si-Si	Si-Si-X	Si-X-Si	sum of int. angle [deg.]	ring torsion angle [deg.]
2a	CH_2	*i*Pr	2.393	1.888	97.5	102.7	117.7	517.9	30.6 (7.3-47.1)
4a	NC_6H_{11}	*i*Pr	2.402	1.760	96.2	106.1	125.6	530.1	20.1 (8.3-27.3)
4b	"	$tBuCH_2$	2.397	1.775	94.0	103.7	123.2	518.6	28.4 (2.0-43.5)
4c	"	$tBuCH_2$	2.402[a]	1.767	94.4	104.1	124.4	521.2	27.0 (5.8-38.9)
		*i*Pr	2.372[b]						
6a	O	*i*Pr	2.392	1.646	95.3	102.0	133.6	528.1	23.0 (9.8-32.1)
6b[c]	"	$tBuCH_2$	2.414	1.631	92.9	103.3	132.3	524.7	24.6 (7.6-33.3)
E[d]	SiR_2	*i*Pr	2.422	2.422	101.9	101.9	101.9	509.5	--
H[e]	$GePh_2$	*i*Pr	2.414	2.434	106.0	102.5	110.5	527.5	22.7 (2.9-34.5)
I[e]	"	$tBuCH_2$	2.414	2.449	102.3	100.3	109.7	514.9	32.3 (14.1-51.7)

[a] Average value of the distances of Si(1)−Si(2) and Si(3)−Si(4). [b] Distance Si(2)−Si(3). [c] Average value from molecules A and B. [d] Ref.[14] [e] Ref.[11]

pyl groups in each set. Comparison of the four angles between the two ring sets identifies some interesting features. The sizes of the corresponding angles fall in the order: Si−N−Si (109.5°, **3a**; 108.7−109.3°, **3b−d**) > Si−Si−N (88.0°, **3a**; 85.9−86.5°, **3b**) > Si−Si−Si (74.5°, **3a**; 74.0−74.3°, **3b−d**). This trend is also observed in the five-membered Si_4N rings of **4a−c**. Interestingly, it could be shown that all the nitrogen atoms in **3** and **4** were of almost sp^2 geometry, from the sums (359.8−360°) of the three angles around the nitrogen atoms, as has also been shown in various silylamines[13] and a calculated cycle $[H_2Si]_3NH$.[6a]

The Si_3O cycle in **5b** and the Si_4O cycles in **6a** and **6b** are almost planar (dihedral angle 3°) and a slightly distorted envelope (dihedral angle 23°−25°), respectively, but **6b** has a distorted half-chair form. The Si−Si bond length in **5b** is 2.433 Å, which is the longest in all the Si_3X rings and considerably longer than that (2.409 Å) in the related cyclotetrasilane **B**. The long Si−Si distance in the small-membered rings is reminiscent of the fact that the presence of the bulky substituents on the highly strained planar Si_3O ring should result in remarkably stretched Si−Si distances, as has been discussed previously for cyclosilanes $[R_2Si]_n$ (n = 3, 4) bearing bulky substituents such as Me_3Si and *t*Bu groups.[7f] The Si−Si bond lengths in **6a** and **6b** are 2.392−2.414 Å, which is comparable with those (2.393−2.402 Å) in the other Si_4X rings of **2** and **4** in Table 14. It is of interest to note that the longer Si−Si bond length in **6b**, relative to those in **6a** and in the other heterosilacyles Si_3X, is similar to the situation in the five-membered rings **E**, **H**, and **I**. The Si−O bond lengths in **5b**, **6a**, and **6b** are in the 1.631−1.656 Å range, around the typical values of 1.64±0.03 Å.[13] The distance (1.656 Å) in **5b** is slightly short relative to those (1.663−1.721 Å) in the similar four-membered compounds cyclo-1,3-disiloxanes $[R_2SiO]_2$.[15] The Si−Si−Si bond angles in **5b**, **6a**, and **6b** are 68.2, 95.3, and 92.9°, respectively, and are the smallest in each set of the two types of rings (68.2−90.4°, Si_3X; 92.9−106.0°, Si_4X), as seen in Tables 13 and 14. Surprisingly, the angle (68.2°) in **5b**, with a planar structure, is unusually small and much closer to the inner angle (60°) of a three-membered ring rather than that (90°) of a planar four-membered one. This compound may thus have quite large angular and Pitzer strains, for which supporting results were obtained by theoretical calculations of the ring strain energies by the PM3 method (vide infra). The Si−O−Si bond angle in **5b** (111.1°) is comparable with those (106.3 and 112.1°) of the calculated $[H_2Si]_3O$,[6a] respectively. However, the Si−O−Si bond angles (133.6 and 132.3°) for **6a** and **6b** are significantly large compared to those (119.9−124.6°) in calculated $[R_2Si]_4O$ (R = H, Me).

Finally, the Si−Si bond lengths in **A−I** (except for **F**) and **1−6** in Tables 13 and 14 fall in the 2.370−2.433 Å range, and are considerably longer than the sums of the covalent

radii (2.34 Å), suggesting that the four- and five-membered rings are fairly strained because of steric repulsion between the bulky substituents (*i*Pr or tBuCH$_2$) on the silicons and the angular strains.

(2) Geometries

Firstly, the geometrical features show the following behavior with increasing bulkiness of substituent from an isopropyl to a neopentyl group in each pair of heterosilacycles $[R_2Si]_nX$ (R = *i*Pr, tBuCH$_2$; X = CH$_2$, NC$_6$H$_{11}$, O, SiR$_2$, GeR$'_2$) (Tables 13 and 14):

i. The dihedral angles in the four-membered cycles increase (**3a**, **3b**; **A**, **B**; **C**, **D**).

ii. In the five-membered cycles, the ring torsion angles increase (**4a**, **4b**; **6a**, **6b**; **H**, **I**), whereas the sums of the internal angles decrease (**4a**, **4b**; **6a**, **6b**; **H**, **I**).

iii. In all cases, the Si−Si and Si−X bond lengths increase, except for Si−Ge in Si$_3$Ge, Si−Si in Si$_4$N, and Si−X in Si$_4$O cycles.

iv. The Si−Si−Si, Si−Si−X, and Si−X−Si bond angles decrease, except for Si−Si−O in the Si$_4$O cycle.

Consequently, the above results probably reflect the fact that the compounds bearing neopentyl groups release the steric repulsions between the bulky substituents through elongation of the bond lengths and expansion of the dihedral angles or torsion angles, while the compounds carrying isopropyl groups avoid steric repulsion (Pitzer strains) through expansion of the internal bond angles and distortion of the molecular shape. The bond elongation with increasing bulkiness of the substituents on the silicon atoms was also confirmed by the fact that the Si−Si bond lengths in the four- and five-membered $[R_2Si]_3X$ and $[R_2Si]_4X$ are longer − except in only one case (X = SiR$_2$)[14,16] − than those in the corresponding calculated cycles $[R_2Si]_3X$ (R = H, Me, etc., X = SiH$_2$, CH$_2$, NH, O).[6a]

Secondly, the types of heteroatoms X in the four- and five-membered cycles $[R_2Si]_nX$ also affect the geometrical parameters as follows:

i. The dihedral angles vary depending on the different combinations of heteroatom X, substituent R, and ring size; that is, Si$_n$X rings with NC$_6$H$_{11}$ or O as X prefer planar conformations (**3a**, **5b**), while the other silacyles have puckered (n = 3) or distorted conformations (n = 4).

ii. For heterosilacycles $[R_2Si]_nX$ [n = 3, 4; R = *i*Pr, tBuCH$_2$; X = Ge(CH$_2$SiMe$_3$)$_2$, CH$_2$, NC$_6$H$_{11}$, O], as can be seen in Tables 13 and 14, the Si−Si−Si bond angles and Si$^{\alpha}$···Si$^{\alpha'}$ nonbonding distances in Si$_3$X decrease with decreasing atomic radii of the heteroatoms X and Si−X bond lengths, whereas the Si−X−Si bond angles increase. Alternatively, with increasing electronegativity[18] of X, decreases in the Si−Si−Si angles and the Si$^{\alpha}$···Si$^{\alpha'}$ nonbonding distances and increases in the Si−X−Si angles were observed. Interestingly, similar results from calculations for $[H_2Si]_3X$ (X = SiH$_2$, PH, S, CH$_2$, NH, O) have previously been reported by another group of workers,[19] who explained their results in terms of a concept, the σ-bridged-π-bonding concept, by which the structural properties were correlated with the electronegativities[18] of the heteroatoms X in the rings. Thus, if this idea is applicable to the current systems for explaining the geometrical properties of such types of small rings, the results shown in Tables 13 and 14 seem virtually to substantiate this concept for the relationship between parameters such as the electronegativity of X, the Si−X bond length, and the Si−X−Si angle.

In terms of the molecular structures of heterosilacycles $[R_2Si]_nX$ (n = 3, 4; R = *i*Pr, tBuCH$_2$; X = CH$_2$, NC$_6$H$_{11}$, O) (**1−6**), it is of considerable interest to discuss the molecular shapes on the basis of the steric repulsions arising from the bulky substituents on the ring silicon atoms and the steric requirements around the heteroatoms X, including their atomic sizes. Scheme 3 shows schematic diagrams of four-membered silacycles consisting of X = CH$_2$, NC$_6$H$_{11}$, O (see Table 13). Silacycles **3a** (X = NC$_6$H$_{11}$; R = *i*Pr) and **5b** (X = O; R = tBuCH$_2$) are planar rings, while **1b** (X = CH$_2$; R = tBuCH$_2$) and **3b−d** (X = NC$_6$H$_{11}$; R = tBuCH$_2$) are folded ones. The results show that when bulky neopentyl groups (steric substituent constant, Es = −1.74)[17] are attached to the two α-silicon atoms (**1b**, **3b−d**, **5b**), heterosilacycle **5b** containing (the smallest) oxygen (covalent atomic radius, 0.66 Å) as X (or X group), is planar, whereas the other silacycles, containing nitrogen (0.70 Å; **3b−d**) and carbon (0.77 Å; **1b**), are folded. However, in **3a**, which contains the medium-sized nitrogen (0.70 Å) as X and less bulky isopropyl substituents (Es = −0.47[17]) on the α-silicon atoms, the ring shape is also planar. In addition, the strongly electronegative X atoms, such as X = O (En = 3.50[18]) and N (En = 3.07[18]) in silacycles **3a−d** and **5b** strongly attract the neighboring silicon atoms (En = 1.74[18]) to produce an Si−X bond length shorter than that calculated on the basis of the normal covalent radii of silicon and X when there is a large electronegativity difference between them.[19] Furthermore, so-called (p−d)π bonding produced by back-donation of the lone-pair electrons from X to the d-orbitals of α-silicon atoms is also possible. From these observations, it is thus reasonable to consider that the ring shapes of the heterosilaycles may be attributable to the result of a compromise between parameters: steric repulsions due to the congestion imposed by the bulky substituents on the silicon atoms, especially α-silicon atoms, the steric requirement around the heteroatoms X (or X groups) in Si−X−Si systems, the ring strain energies, and the electronegativity differences between heteroatom X (or heteroatom group) and silicon.

For five-membered rings $(R_2Si)_nX$ (n = 4; R = *i*Pr; tBuCH$_2$) (**2**, **4**, **6**), on the other hand, detailed investigation of the molecular shapes is apparently necessary to explain their structural features in Table 14 fully.

^{29}Si NMR Spectra

The ^{29}Si NMR spectroscopic data for **1−6** are summarized in Table 15, together with those for the related compounds **A−I** (except for **F**). Various features relating to variation in ring size, heteroatom X, silicon atom (Si$^{\alpha}$ or Si$^{\beta}$), and substituents on the silicon atoms [see Scheme 1, (a)−(e)] are observed, as follows:

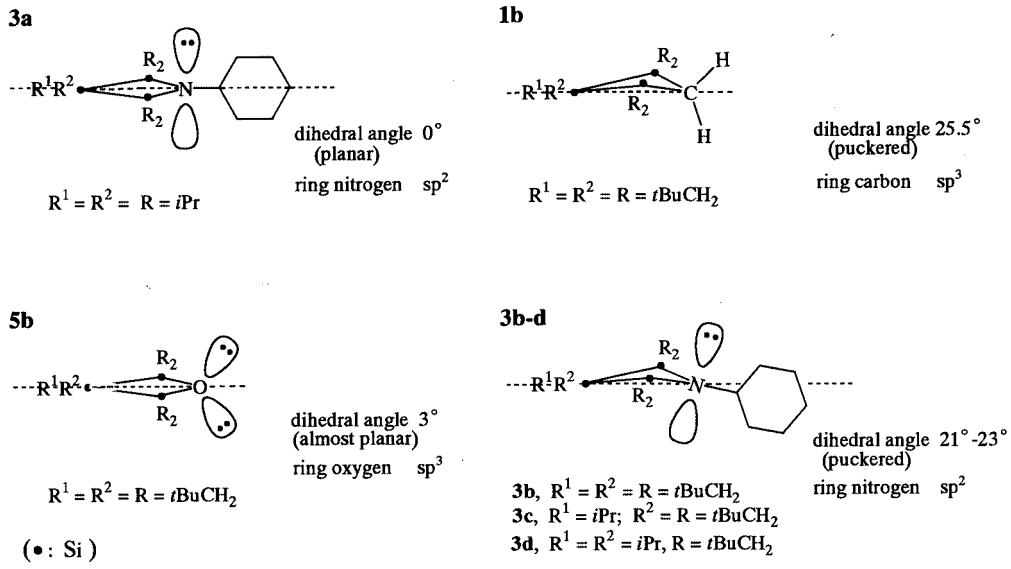

Scheme 3. Schematic diagrams of four-membered heteroatom-containing silacycles **1b**, **3a**−**d**, and **5b** (side views)

1) The resonances for the α-silicon atoms attached to the heteroatoms X are shifted downfield by a deshielding effect due to the electronegative atom X, and − as shown in Figure 1 − the larger the electronegativity (*En*)[18] of X, the lower the field of the chemical shifts.

2) The resonance for the β-silicon atoms generally occurs at higher fields than those for the α-silicon atoms, and there is no relationship between the chemical shift of the β-silicon atoms and the electronegativity[18] of X.

3) In the $[(iPr)_2Si]_nX$ and $[(R^1R^2Si)_n\{(tBuCH_2)_2Si\}_2]X$ types (n = 1, 2), the resonances for the α- and β-silicon atoms appeared at higher fields with increasing ring size, due to a shielding effect with decreasing ring strain, as has previously been shown in various cyclosilanes.[20]

4) In each system of Si_nX cycles, the resonances for both α- and β-silicon atoms of the compounds bearing neopentyl groups are shifted to higher fields than those bearing isopropyl groups, since the silicon atom at the γ-position from the terminal methyl carbon atom in an $SiCH_2C(CH_3)_3$ group is subject to a high-field shielding effect due to the terminal carbon atom.[21]

Interestingly, it can be seen from Table 15 that the trend towards an increasing deshielding effect on the Si^{α} chemical shifts with increasing electronegativity[18] of X is substantially present, regardless of the presence or absence of a substituent on the heteroatom X. Indeed, as shown in Figure 1, the chemical shifts of the Si^{α} atoms in each series showed a good linear correlation with the electronegativity[18] of the heteroatom X, with good correlation coefficients (γ = 0.95−0.99). This is the first example in which a good linear correlation of δSi^{α} with the electronegativity[18] of X in the $[R_2Si]_nX$ cycles has been found.

Table 15. ^{29}Si NMR spectroscopic data for $[(R^1R^2Si)_p(R_2Si)_2]X$[a] and related compounds

ring size	p	$R^1;R^2$	X	compd	δSi [ppm][b] Si^{α}	Si^{β}	ref.
4	1	$(iPr)_2$	SiR_2	**A**[c]	-5.5	-5.5	[7f]
			$Ge(CH_2SiMe_3)_2$	**C**[c]	5.8	2.2	[10]
			CH_2	**1a**	9.1	5.1	this work
			NC_6H_{11}	**3a**	17.2	-8.6	"
			O	**5a**[c]	31.4	11.3	"
		$(tBuCH_2)_2$	SiR_2	**B**[c]	-23.6	-23.6	[16]
			$Ge(CH_2SiMe_3)_2$	**D**[c]	-11.8	-23.5	[10]
			CH_2	**1b**	-4.0	-18.6	this work
			NC_6H_{11}	**3d**	7.7	-8.6	"
			NC_6H_{11}	**3c**	8.5	-18.0	"
			NC_6H_{11}	**3b**	9.5	-30.9	"
			O	**5b**	29.4	-22.1	"
5	2	$(iPr)_2$	SiR_2	**E**[c]	-14.8	-14.8	[14]
			$GePh_2$	**H**[c]	-12.1	-13.8	[11]
			$Ge(CH_2SiMe_3)_2$	**G**[c]	-10.7	-12.5	"
			CH_2	**2a**	1.9	-18.6	this work
			NC_6H_{11}	**4a**[c]	1.8	-34.8	"
			O	**6a**	15.7	-20.4	"
		$(tBuCH_2)_2$	$GePh_2$	**I**[c]	-24.0	-29.0	[11]
			CH_2	**2b**	-8.7	-39.9	this work
			NC_6H_{11}	**4c**	0.0	-26.0	"
			NPr	**4d**	2.3	-42.5	"
			NC_6H_{11}	**4b**	2.7	-42.2	"
			O	**6b**	13.6	-44.3	"

[a] R^2 = *i*Pr or $tBuCH_2$. [b] In $CDCl_3$. [c] In C_6D_6.

Electronic Spectra

The UV spectra for $[R_2Si]_nCH_2$ (**1**, **2**), $[R^1R^2Si]_nNR^3$ ($R^3 = C_6H_{11}$ or Pr) (**3**, **4**), and $[R^1R^2Si]_nO$ (**5**, **6**) are listed in Table 16. In the UV spectra of **1a** and **1b** and of **2a** and **2b**, the longest-wavelength absorptions occur at λ = 234, 231 and 261, 254 nm, respectively, with varying extinction coefficients. The absorption maxima for the Si_3C cycles (**1**) consisting of peralkylated ring silicon atoms are substantially different from those (λ = 502−538 nm) for known Si_3C cycles with rather particular substituents,[3b][3c] such as trisilacyclobutaimines $[tBu_2Si]_3C{=}NAr$. The absorption maxima of Si_4C (**2**) occur in almost the same region as that (λ = 258 nm) of peralkylated compound $[Me_2Si]_4CH_2$[3j] and are fairly different from that (λ = 443 nm) of perphenylated tetrasilacyclopentaimine $[Ph_2Si]_4C{=}NPh$[3f] and that (λ = 325 nm) of partially phenylated allenic tetrasilacy-

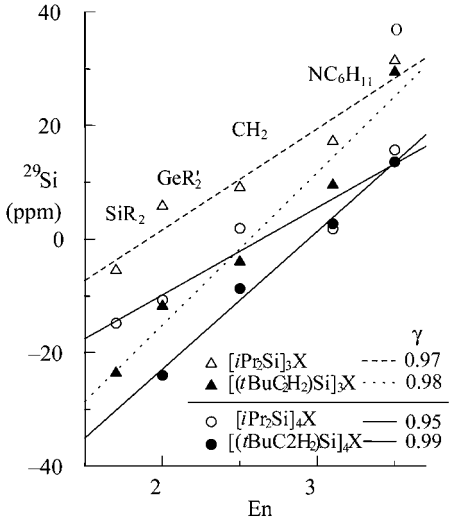

Figure 1. Correlation of $^{29}Si^{\alpha}$ chemical shifts with the electronegativities (*En*, see ref.[18]) of heteroatom X in $[R_2Si]_nX$ (n = 3, 4; R = *i*Pr, *t*$BuCH_2$)

clopentane $[Me_2Si]_4C{=}C{=}CPh_2$.[3e] It is worth noting that the UV absorption spectra of **1** are the first results for the peralkylated four-membered Si_3C cycle, since no such spectroscopic data have been described even for the only known peralkylated compound $[Me_2Si]_3CH_2$.[3a]

Table 16. UV data for $[R_2Si]_nX$ and related compounds

ring size	n	X	R	compd	λ_{max} / nm [ε / $mol^{-1}dm^3 cm^{-1}$][a]
4	3	CH_2	*i*Pr	**1a**	234 (8800)
			t$BuCH_2$	**1b**	231 (9400)
		NC_6H_{11}	*i*Pr	**3a**	233 (12000)
			t$BuCH_2$	**3b**	237 (10000)
			*i*Pr, *t*$BuCH_2$	**3c**	236 (8800)
			*i*Pr, *t*$BuCH_2$	**3d**	236 (10500)
		O	*i*Pr	**5a**	247 (10100), 203 (13600)
			t$BuCH_2$	**5b**	250 (11400), 205 (12000)
			*i*Pr, t-$BuCH_2$	**5c**	245 (11000), 213 (7400)
		SiR_2	*i*Pr	**A**	290 (200)[b]
			t$BuCH_2$	**B**	286 (440)[c]
		$Ge(CH_2SiMe_3)_2$	*i*Pr	**C**	300 (320)[d]
			t$BuCH_2$	**D**	286 (590)[d]
5	4	CH_2	*i*Pr	**2a**	261 (1100)
			t$BuCH_2$	**2b**	254 (1500), 233sh (6500)
		NC_6H_{11}	*i*Pr	**4a**	252sh (1600)
			t$BuCH_2$	**4b**	252sh (4100)
			*i*Pr, *t*$BuCH_2$	**4c**	252sh (2800)
		NPr	*t*$BuCH_2$	**4d**	252sh (3700)
		O	*i*Pr	**6a**	260sh (1800), 239 (9800) 220 (15500), 203 (18400)
			t$BuCH_2$	**6b**	255sh (3900), 242 (5800) 217 (16400)
		SiR_2	*i*Pr	**E**	274 (1700), 265 (1800)[e,f]
			*i*Bu	**F**	260sh (1500)[b]
		$Ge(CH_2SiMe_3)_2$	*i*Pr	**G**	280sh (1100), 262 (2000)[g]
		$GePh_2$	*i*Pr	**H**	280sh (5700), 252 (16000) 240 (18000)[g]
			t$BuCH_2$	**I**	280sh (7600), 245 (19000)[g]

[a] In *c*-C_6H_{12}. [b] Ref.[7d] [c] Ref.[16] [d] Ref.[10] [e] See also ref.[14] [f] Our data. [g] Ref.[7d]

The *N*-substituted four- and five-membered cycles **3** and **4** showed the longest-wavelength absorption bands at λ = 233−240 nm and 252 nm (sh), respectively. The absorption (252 nm) for **4** occurred at a longer wavelength region than that (235 nm) for $[Me_2Si]_4NMe$,[6b−6d] but shorter than that (282 nm) for $[Ph_2Si]_4NR^3$ (R^3 = Me, Et).[6e]

In the UV spectra of the *O*-substituted four- and five-membered compounds **5** and **6**, the longest-wavelength absorption bands occurred at λ = 245−250 and 255−260 nm, respectively. The absorption maxima for the Si_4O cycles (**6**) are comparable with those (λ = 253−258 nm) for $[Me_2Si]_4O$,[6d] $[Ph_2Si]_4O$,[6e] and $[Me(tBu)Si]_4O$.[5d] The UV data for the four-membered compounds **3** and **5** are the first examples for the Si_3N and Si_3O ring systems, respectively.

The UV data for **1−6** in Table 16, together with those for the related compounds **A−I**, showed various interesting features, as follows:

i. Little difference was observed in the UV data for $[iPr_2Si]_nX$ and $[(tBuCH_2)_2Si]_nX$ of the same ring size.

ii. With respect to the longest-wavelength absorption bands, compounds **1−6** and **A−I** could be roughly classified by a combination of ring size and heteroatom X into four groups: (a) $[R_2Si]_3X$ [X = SiR_2, $Ge(CH_2SiMe_3)_2$] (**A−D**), λ = 280−300 nm; (b) $[R_2Si]_3X$ (X = CH_2, NC_6H_{11}, O) (**1**, **3**, **5**), λ = 230−250 nm; (c) $[R_2Si]_4X$ (X = SiR_2, GeR'_2; R′ = CH_2SiMe_3, Ph) (**E**, **G−I**), λ = 270−300 nm; (d) $[R_2Si]_4X$ [X = CH_2, NR^3 (R^3 = C_6H_{11}, Pr), O] (**2**, **4**, **6**), λ = 250−260 nm. Compounds belonging to the same group showed absorption bands in almost the same region with nearly the same molar extinction coefficients, regardless of the nature of X and the substituents on the silicon atoms.

iii. As the ring size increased, the absorption maxima for the *Ge*-substituted compounds **C−D** and **G−I** hypsochromically shifted by 8−10 nm with increased extinction coefficients, as expected by analogy with the peralkylcyclosilanes such as $[R_2Si]_n$ (R = Me[22a,22b] and Et[22c]), while those for the *C*-, *N*-, and *O*-substituted compounds **1−6** bathochromically shifted by 10−20 nm with decreased extinction coefficients. This trend resembles that observed with increasing chain length for linear permethylpolysilanes $Me(Me_2Si)_nMe$,[23] rather than the cyclosilanes[22] mentioned above. Similarly, bathochromic shifts with increasing ring size have previously been observed for the *N*-substituted compounds $[Me_2Si]_nX$ (n = 4−6).[6b]

iv. The molar extinction coefficients (ε = 200−4100 $dm^3cm^{-1}mol^{-1}$) for compounds **A−I**, **2**, **4**, **6**, containing one germanium or four silicon atoms in the ring systems, were very small relative to those (ε = 8800−12000 $dm^3{\cdot}cm^{-1}{\cdot}mol^{-1}$) for **1**, **3**, and **5**, containing three silicon atoms. The large difference in the ε values between the two sets of ring systems may be due to differences in the forbidden σ−π* or allowed σ−σ* transitions[1a][3j] (vide infra).

Ring Strain Energies by Theoretical Calculation

The ring strain energies of homosilacycles or silicon cluster compounds are a very interesting subject, not only experimentally but also theoretically. We have previously experimentally determined the ring strain energies for a series of peralkylated homosilacycles $[R^1R^2Si]_n$ as 41, 23, 6, and 0 kcal/mol for n = 3−6, respectively.[7e] From the theoretical perspective, on the other hand, the homodesmotic ring strain energies for $(SiH_2)_4$ and $(SiH_2)_5$ at HF (Hartree−Fock) or MP2 levels with the basis sets of double

zeta plus polarization functions quality were calculated to be ca. 17.0 and 6.0 kcal/mol, respectively.[24] Similar results (18.7 and 5.7 kcal/mol) have been obtained at the higher MP4SDTQ/6-31G** level.[25] The calculated values thus seem to be slightly underestimated for the four-membered ring, although the data for the five-membered ring agree well with the above experimentally determined values.

Although some theoretical studies on the types of homosilacycles $(SiH_2)_n$[24,25] mentioned above and on $(SiH_2)_nX$ (X = PH and S)[19,26] are thus available, alkyl-substituted homosilacycles $(SiR_2)_n$ and alkyl-substituted heteroatom-containing silacycles have not so far been reported. In a preliminary study,[27] we estimated the ring strain energies for the alkylated four- and five-membered heterosilacyles $[R_2Si]_nX$ [R = Me, *i*Pr; n = 3, 4; X = CH_2, NMe, N(*i*Pr), O, SiH_2], on the basis of the homodesmotic reaction energies.[28] The magnitudes of the calculated strain energies for the series R = *i*Pr, listed in Table 17, were found to be in the order: n = 3: X = O (**5a**, 12.8 kcal/mol) > CH_2 (**1a**, 8.7) > SiH_2 (8.1) > N(*i*Pr) (6.4) > NMe (2.2); n = 4: X = N(*i*Pr) (11.4) > O (**6a**, 8.3) > SiH_2 (3.9) > CH_2 (**2a**, 3.1) > NMe (−2.1). In the four-membered cycle with SiH_2 as X, it was shown that the PM3 strain energy (8.1 kcal/mol) was much less than the above result (18.7 kcal/mol) obtained by the ab initio method,[25] and also the experimentally determined one (23 kcal/mol). The strain energies calculated for the four-membered rings are much larger than those for the five-membered rings for all kinds of heteroatom (or heteroatom group) X except for X = N(*i*Pr), in which the two kinds of silacycles are reversed in the magnitude of their strain energies. This may be explained in terms of the steric repulsions between the bulky groups including the Si−N(R^3)−Si system (R^3 = *i*Pr; see Table 17, footnote) in the Si_4N cycle, as such an effect is apparently more severe in the five-membered cycle than in the four-membered one, as shown and discussed previously for homosilacycles.[7f] This order of the magnitude in the two series of silacycles seems to be reasonable, although more advanced calculations are necessary.[27] In the four-membered rings, it is noteworthy that the strain energy (12.8 kcal/mol) for **5a** (X = O) is the largest and that the results agree well with prediction from the structural features of this molecule, that is, the highly strained conformation, as shown in Table 13 and discussed in the previous section. For the silacycles with X = CH_2 and SiH_2 as X, the strain energies of Si_3X (8.7, 8.1 kcal/mol) and Si_4X (3.1, 3.9) are fairly close to each other, while those for Si_3X and Si_4X cycles where X = NMe (2.2, −2.1, respectively) are the smallest. However, the considerable strain energy for Si_3X, X = N(*i*Pr) (6.4 kcal/mol) is of interest, because the conformation of the silacycle, including the steric requirements around the Si−N(R^3)−Si system, seems to be similar to that of X = NC_6H_{11} (**3a**, see also Table 17, footnote). The large strain energy calculated for Si_4X (X = O, **6a**) (8.3 kcal) may also be in agreement with the experimental results shown in Table 2, in which the conformation, consisting of the relatively small angles Si−Si−Si (95°) and Si−Si−O (102°), the large angle Si−O−Si (134°), the short distance Si−O (1.65 Å), and the small ring-torsion angle (23°), would be a fairly strained molecule. It is worthwhile to note that a similar consideration may be applicable to the large strain energy (11.4 kcal/mol) for the heterosilacycles containing X = N(*i*Pr) if the X group can accommodate the NC_6H_{11} group of **4a** (see Table 17, footnote).

Table 17. Estimated strain energies [kcal/mol] of $[R_2Si]_nX$ at PM3 level

ring size	n	X	R: Me	R: *i*Pr
4	3	CH_2	7.9	8.7 (**1a**)
		NMe	9.0	2.2
		N(*i*Pr)[a]	...	6.4
		O	10.8	12.8 (**5a**)
		SiH_2	5.1	8.1
5	4	CH_2	0.9	3.1 (**2a**)
		NMe	-2.0	-2.1
		N(*i*Pr)[a]	...	11.4
		O	-0.9	8.3 (**6a**)
		SiH_2	0.5	3.9

[a] For convenience, the bulkiness of the two β-carbon atoms of the isopropyl group is assumed to be close to those of the cyclohexyl group; polar substituent constant σ*(*i*Pr) = −0.190, σ*(C_6H_{11}) = −0.15 (see ref.[17])

Oxidation Potentials

The oxidation potentials (E_{pa} vs. SCE) of the homo- and heterosilacycles were determined by cyclic voltammetry in MeCN or CH_2Cl_2. The results are summarized in Table 18[7h,29] and Table 19, respectively, together with those for the related compounds **A**−**I** (except for **E**). Firstly, it should be noted that this is the first report describing the oxidation potentials for silacycles containing a heteroatom in the ring system $[R_2Si]_nX$ (X = CH_2, O, NR^3, GeR'_2). The silacycles also gave irreversible voltammograms similar to those obtained for the homosilacycles, as shown in the previous work,[7h] suggesting the formation of their unstable cation-radicals produced from the starting silacycles. Interestingly, the oxidation potentials thus obtained from the four- and five-membered silacycles **1**, **3**, **5**, **A**−**D** and **2**, **4**, **6**, **F**−**I** roughly fall into nearly the same potential ranges as found for the homosilacycles Si_4 and Si_5[7h] in the two solvents. Thus, the potentials for the Si_3X rings were 0.8−1.0 V in MeCN and 0.96−1.24 V in CH_2Cl_2, while those for the Si_4X rings were 1.0−1.24 V in MeCN and 1.16−1.53 V in CH_2Cl_2. As described in the previous work,[7h] solvation of the cation radicals produced by the oxidations may account for the lower potentials in MeCN than in CH_2Cl_2 for **1**−**6**. Furthermore, it is also apparent from Table 19 that the potentials for the Si_3X system decreased relative to those for the Si_4X system in each solvent system. The results are in accord with the trend of the oxidation potentials in a series of homosilacycles $[R^1R^2Si]_n$ (n = 3−7).[7h,29] The silacycles of smaller ring size have larger ring strain energies and more strongly electron-donating natures than those with larger ring sizes.[7e] It was thus found that the oxidation potentials were primarily affected by the ring size, regardless of the types of heteroatom X and the substituents on the silicon

atoms, and − in addition − the presence or absence of a substituent on the heteroatom X.

Table 18. Oxidation and ionization potentials and HOMO and LUMO levels for homosilacycles $[R^1R^2Si]_m$ and related silacycles

no.	m	compd	Epa [V vs. SCE][a] CH_3CN	Epa [V vs. SCE][a] CH_2Cl_2	λ_{max}[b] [nm]	Ip, HOMO [eV] [c]	Ip, HOMO [eV] [d]	LUMO[e] [eV]	E_T[f] [eV]
1	3	$[(tBuCH_2)_2Si]_3$	0.44	0.72	310sh	-6.90[g]		-2.90	4.00
		"		0.58[h]					
2		$[(tBuCH_2)_2Si]_2GeR'_2$[i]	0.37	0.57	312sh		-6.78	-2.81	3.97
3	4	$[iPr_2Si]_4$	1.00	1.24	290sh	-7.22[h]		-2.94	4.28
4		$[sBu_2Si]_4$	1.10	1.23	290sh		-7.44	-3.16	4.28
5		$[Me(tBu)Si]_4$	0.94	1.08	300	-7.42[j]		-3.29	4.13
		"		1.21[h]					
6		$[(tBuCH_2)_2Si]_4$	1.10	1.19	298sh[l]		-7.40	-3.06	4.34
7		$[(Me_3Si)_2Si]_4$		1.11[h]	286[k]	-7.10[g]		-2.94	4.26
8		$[iPr_2Si]_3GeR'_2$[i]	0.80	0.96	300		-7.17	-3.05	4.12
9		$[(tBuCH_2)_2Si]_3GeR'_2$[i]	0.80	0.97	286		-7.18	-2.84	4.34
10	5	$[Me_2Si]_5$	1.08	1.26	275	-7.94[m]		-3.43	4.51
		"		1.54[h]					
11		$[Et_2Si]_5$	1.48	1.36[h]	265sh		-7.57	-2.89	4.68
12		$[Pr_2Si]_5$	1.42	1.45	260		-7.66	-2.89	4.87
13		$[Bu_2Si]_5$	1.40	1.30	262		-7.51	-2.78	4.73
14		$[iBu_2Si]_5$	1.36	1.38	260sh		-7.59	-2.68	4.91
15		$[iPr_2Si]_4GeR'_2$[i]	1.04	1.23	280sh		-7.44	-3.01	4.43
16	6	$[Me_2Si]_6$	1.45	1.65	258sh	-7.79[m]		-2.98	4.81
		"		1.54[h]					
17		$[PrMeSi]_6$	1.22		257sh				
18	7	$[Pr_2Si]_7$	1.40	1.40	242		-7.61	-2.49	5.12

[a] The first anodic peak potentials; scan rate, 250 mV/s; see also ref.[7h] [b] Longest-wavelength absorption band. [c] Reported values from UPS measurements. [d] Calculated values based on the regression line (Figure 2) obtained from the relationship between the ionization (UPS) and oxidation potentials (CV, E_{pa} in CH_2Cl_2) determined experimentally for runs number 1, 3, 5, 7, 10, and 16, respectively. [e] Values calculated by using the HOMO levels and the transition energies obtained from the longest-wavelength absorption bands. [f] Transition energy. [g] Ref.[31] [h] Ref.[29]; scan rate, 500 mV/s. [i] R′ = Me_3SiCH_2. [j] Ref.[32] [k] Ref.[16] [l] Ref.[34] [m] Ref.[35]

Table 19. Oxidation and ionization potentials and HOMO and LUMO levels for four- and five-membered silacycles $[R_2Si]_nX$

ring size	n	X	R	compd	Epa [V vs. SCE][a] CH_3CN	Epa [V vs. SCE][a] CH_2Cl_2	HOMO[b] [eV]	LUMO[c] [eV]	E_T[d] [eV]
4	3	CH_2	iPr	1a	0.86	1.00	-7.21	-1.91	5.30
		"	tBuCH$_2$	1b	0.85	1.06	-7.27	-1.90	5.37
		NC_6H_{11}	iPr	3a	0.94	1.19	-7.40	-2.08	5.32
		"	tBuCH$_2$	3b	0.89	1.04	-7.25	-2.02	5.23
		"	iPr, tBuCH$_2$	3c	0.94	1.19	-7.40	-2.15	5.25
		"	iPr, tBuCH$_2$	3d	0.94	1.22	-7.43	-2.17	5.26
		O	iPr	5a	0.86	1.05	-7.26	-2.24	5.02
		"	tBuCH$_2$	5b	0.97	1.20	-7.41	-2.45	4.96
		SiR_2	iPr	A	1.00	1.24	-7.22[e]	-2.94	4.28
		"	tBuCH$_2$	B	1.00	1.19	-7.40	-3.06	4.34
		$Ge(CH_2SiMe_3)_2$	iPr	C	0.80	0.96	-7.17	-3.03	4.14
		"	tBuCH$_2$	D	0.80	0.97	-7.18	-2.84	4.34
5	4	CH_2	iPr	2a	1.17	1.43	-7.64	-2.89	4.75
		"	tBuCH$_2$	2b	1.02	1.20	-7.41	-2.53	4.88
		NC_6H_{11}	iPr	4a	1.11	1.29	-7.50	-2.58	4.92
		"	tBuCH$_2$	4b	1.05	1.16	-7.37	-2.45	4.92
		"	iPr, tBuCH$_2$	4c	1.07	1.28	-7.49	-2.57	4.92
		NPr	tBuCH$_2$	4d	1.07	1.23	-7.43	-2.51	4.92
		O	iPr	6a	1.22	1.34	-7.55	-2.78	4.77
		"	tBuCH$_2$	6b	1.08	1.23	-7.44	-2.57	4.87
		SiR_2	iBu	F	1.36	1.38	-7.59	-2.68	4.91
		$Ge(CH_2SiMe_3)_2$	iPr	G	1.04	1.23	-7.44	-3.01	4.43
		$GePh_2$	iPr	H	1.27	1.53	-7.73	-3.30	4.37
		"	tBuCH$_2$	I	1.13	1.34	-7.55	-3.12	4.43

[a] The first anodic peak potentials; scan rate, 250 mV/s; see also ref.[7h] [b] Values calculated using the regression line (Figure 2) obtained from the experimental data of the oxidation (E_{pa}, CH_2Cl_2) and ionization potentials (Table 18). [c] Values calculated by using the HOMO levels and the transition energies obtained from the longest-wavelength absorption bands (Table 16). [d] Transition energy. [e] Ref.[31]

Molecular Frontier Orbitals

Generally, it is well known that oxidation potentials obtained by cyclic voltammetry (CV) for various compounds are linearly correlated to their ionization potentials,[30] which are useful for evaluation of HOMO levels. Accordingly, the oxidation potentials for this series of heteroatom-containing silacycles are applicable to estimation of their HOMO levels, from which their LUMO levels can also be estimated.

(1) Observed Results

Firstly, in order to determine the HOMO levels for a series of homosilacyles, we obtained a regression line for the relationship, with a good correlation coefficient (γ = 0.86 in Figure 2), between the reported ionization potentials (eV) of some homosilacycles measured by photoelectron spectroscopy (PES)[31−33,35] and their oxidation potentials (E_{pa}, in V vs. SCE in CH_2Cl_2) determined by the CV method, as listed in Table 18 (numbers 1, 3, 5, 7, 10, and 16). Interestingly, it should be pointed out that, in the current study, the E_{pa} value of $(Me_2Si)_5$ was shown to be 1.26 V (number 10), whereas the reported value is 1.54 V.[29] Although a better correlation (γ = 0.92) can be obtained if the former value is disregarded, the reason why the relatively large discrepancy occurred could not be clarified and remains to be investigated.

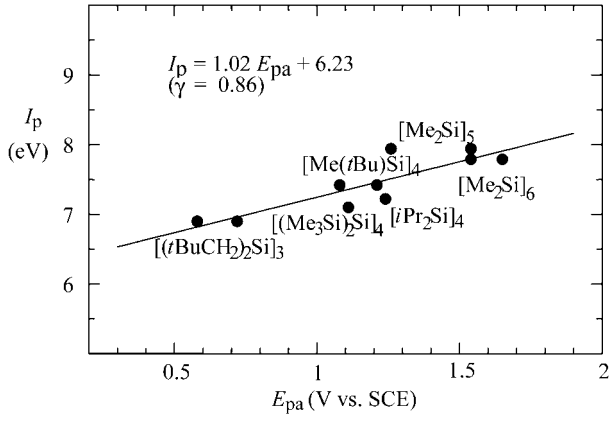

Figure 2. Correlation of the ionization potentials (PES) with the oxidation potentials (CV) of peralkylated homosilacycles $[R_2Si]_n$ (n = 3−7)

Next, with the aid of the regression line (Figure 2), the frontier HOMO levels of all the homosilacycles $(R_2Si)_m$ were estimated, from the oxidation potentials listed in Table 18, as approximately −6.8, −7.3, −7.7, −7.8, −7.6 eV for m = 3−7 (numbers 1−18), respectively. The

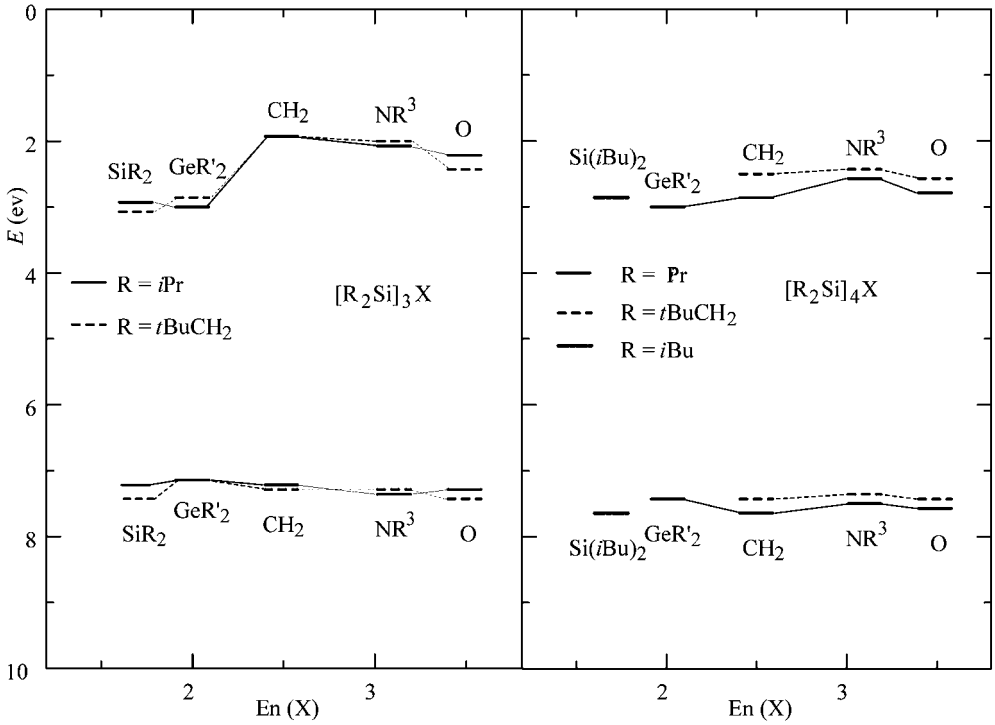

Figure 3. HOMO and LUMO levels for four- and five-membered heteroatom-containing silacycles $[R_2Si]_nX$ (n = 3, 4; R = iPr, tBuCH$_2$)

results clearly exhibit decreasing levels with increasing ring size, except for m = 7, which is similar to that of m = 5. However, the LUMOs of m = 3−6 fall within a narrow range (numbers 1−17, −2.81 to −3.29 eV), and the level for the ring size m = 7 (number 18, −2.5 eV) appears to be slightly higher than those for m = 3−6.

In a similar manner, the two frontier levels for the series of heteroatom-containing silacycles $[R_2Si]_nX$ (R = iPr, tBuCH$_2$; n = 3, 4; X = CH$_2$, O, NR^3, SiR$_2$, GeR$'_2$) were then estimated as listed in Table 19 and shown in Figure 3. Of interest is the fact that, in the four-membered cycles (n = 3), the HOMO levels were found to be very close to each other (ca. 7.2−7.4 eV), due to the close values of their oxidation potentials (E_{pa} = 0.96−1.24 V). The results suggest that the HOMOs of the $[R_2Si]_3X$ series lie at very close levels, probably arising from similar bonding character in the four-membered heterosilacycles at the HOMO levels. For the frontier orbitals of the five-membered cycles Si$_4$X, on the other hand, the HOMO levels are also very close to each other (Figure 3), but, as would be expected from their oxidation potentials, are at slightly lower levels than those for the Si$_3$X cycles.

With regard to the LUMO levels for the Si$_3$X cycles, the experimentally determined results can apparently be classified by the size of the energy gaps (E_T) into two groups: X = CH$_2$, NR^3, O (**1**, **3**, **5**) and X = SiR$_2$, GeR$'_2$ (**A**, **D**), as shown in Table 19 and Figure 3. Interestingly, as can be seen in Figure 4 at the LUMOs, including both the first LUMO and the second LUMO levels, which are in a very narrow range (vide infra), it is likely that the enhanced LUMO levels of the former group in comparison to those of the latter may be attributable to the contribution of the heteroatom (or heteroatom group) X to the frontier orbitals, especially the LUMOs, associated with the conformations due to the four-membered ring systems. In addition, the transition probabilities from the HOMOs to the LUMOs (ε = 8800−12000 dm^3·cm^{-1}·mol^{-1}for **1**, **3**, **5**; "allowed" transition[36]) for the former definitely appear different from those for the latter (ε = 200−590 dm^3·cm^{-1}·mol^{-1} for **A**−**D**; "forbidden" transition[36]), as shown in the longest-wavelength UV absorption bands in Table 16.

For the five-membered Si$_4$X (X = SiR$_2$, GeR$'_2$, CH$_2$, NR^3, O), on the other hand, the LUMOs are close to each other in all ring types, showing lower levels than those seen for the corresponding Si$_3$X, except for X = SiR$_2$. Thus, the contribution of the heteroatom (or heteroatom group) X to the LUMOs mentioned above cannot be observed in Figure 5 in the heterosilacycles containing X = CH$_2$, NR^3, O (**2**, **4**, **6**), which is related to their conformations. The values for the transition probabilities (ε = 1100−4100 dm^{3}cm^{-1}mol^{-1} for **2**, **4**, **6**, **E**, **F**, **G**; "partially allowed" transition[36]) in Table 16 fall in the mid-range between the two cases in the transitions, including compounds **H** and **I** (ε = 5700−7600 dm^{3}cm^{-1}mol^{-1}) which contain phenyl rings that provide resonance effects on the germanium atom in the rings.

From the above observations it should therefore be noted that the concept of a contribution through the heteroatom (or heteroatom group) X in the Si−X−Si systems to the LUMOs derived from theoretical calculations for the

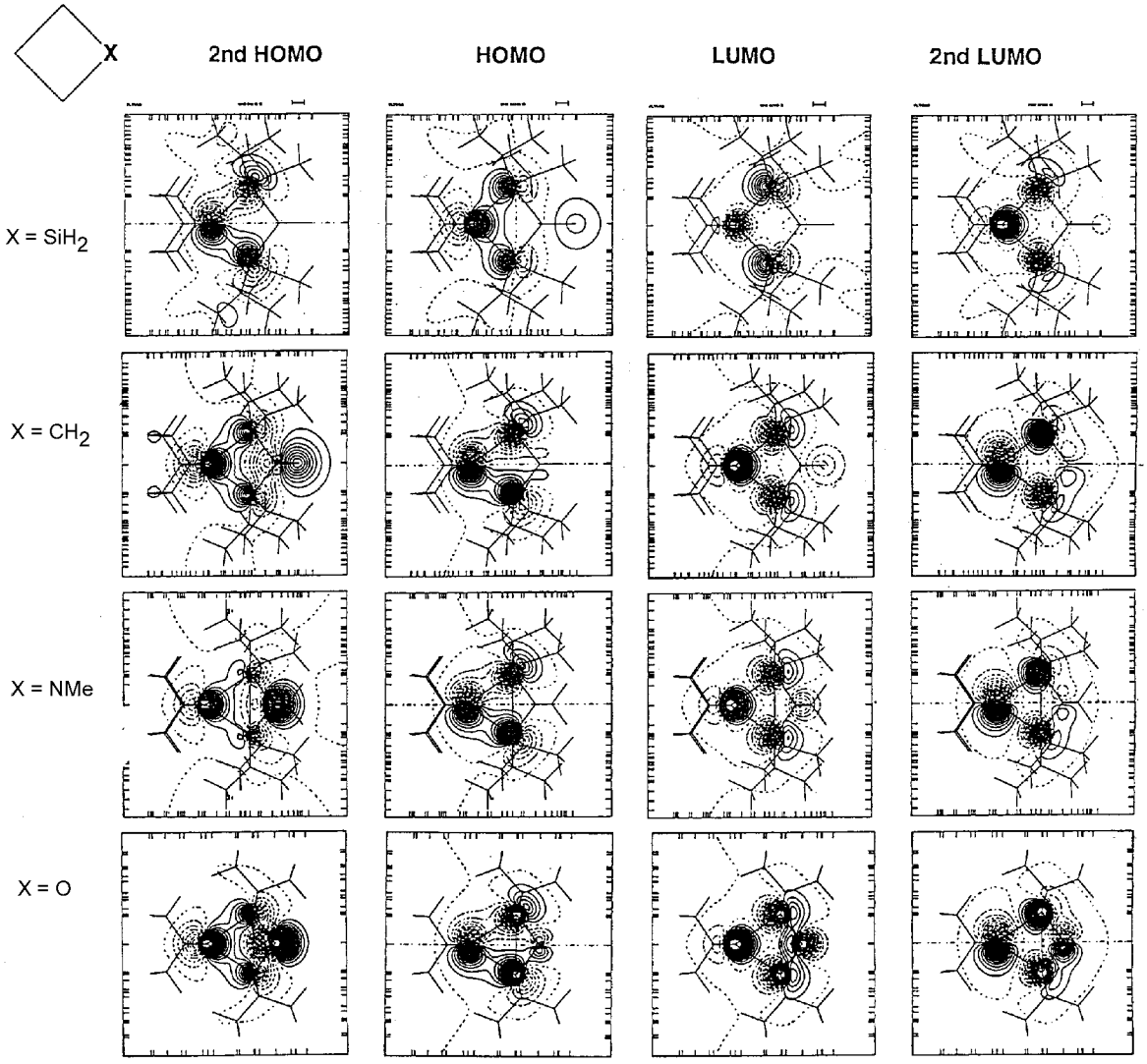

Figure 4. Orbital pictures of the frontier orbitals of $[(i\mathrm{Pr})_2\mathrm{Si}]_3\mathrm{X}$ (X = SiH_2, CH_2, NMe, and O)

HOMOs and LUMOs of the heterosilacycles Si_3X and Si_4X (X = CH_2, NR^3, O) may account for the above experimental results, although detailed studies are necessary.[27]

(2) Theoretical Calculations

The frontier orbital levels determined by PM3 are listed in Table 20. There seems to be no clear trend in the transition energies or energy gaps (E_T) of the molecules of interest. In the case of X = SiH_2, both HOMO and LUMO levels lie slightly lower in energy than in the other compounds with heteroatoms (or heteroatom groups). Both energy levels are almost the same in both sizes of rings, but the energy gaps seem to be slightly smaller in the five-membered rings than in the four-membered ones. Interestingly, the trend of the calculated E_T values in Table 20 for the series of compounds $[(i\mathrm{Pr})_2\mathrm{Si}]_n\mathrm{X}$ [n = 3, 4; X = CH_2, NMe, N(iPr), O, SiH_2] is in good agreement with those for the series of experimental results obtained from the corresponding (or similar) heterosilacycles $[R_2Si]_nX$ [n = 3, 4; X = CH_2 (**1a**; **2a**), NC_6H_{11} (**3a**; **4a**), O (**5a**; **6a**), SiR_2 (**A**; **E**)], respectively (see Table 19 and Figure 3).

The frontier orbitals for the four- and five-membered rings containing X = CH_2, NMe, SiH_2, and O are displayed in Figures 4 and 5, respectively. The orbital levels of the HOMO and the second HOMO, and the LUMO and second LUMO are very close to each other, so that the order of levels can vary depending on the kinds of heteroatom (or heteroatom group). However, the character of the orbitals is independent of the natures of X, as the HOMOs are almost localized on the ring frames. This is also true even if the kinds of substituents are changed. Interestingly enough, it was shown from Figures 4 and 5 that photochemical bond scission in the heteroatom-containing silacycles $[(i\mathrm{Pr})_2\mathrm{Si}]_n\mathrm{X}$ would occur at the Si−Si bonds and not at the Si−X bonds, as the HOMOs and LUMOs have Si−Si bonding and antibonding character, respectively.

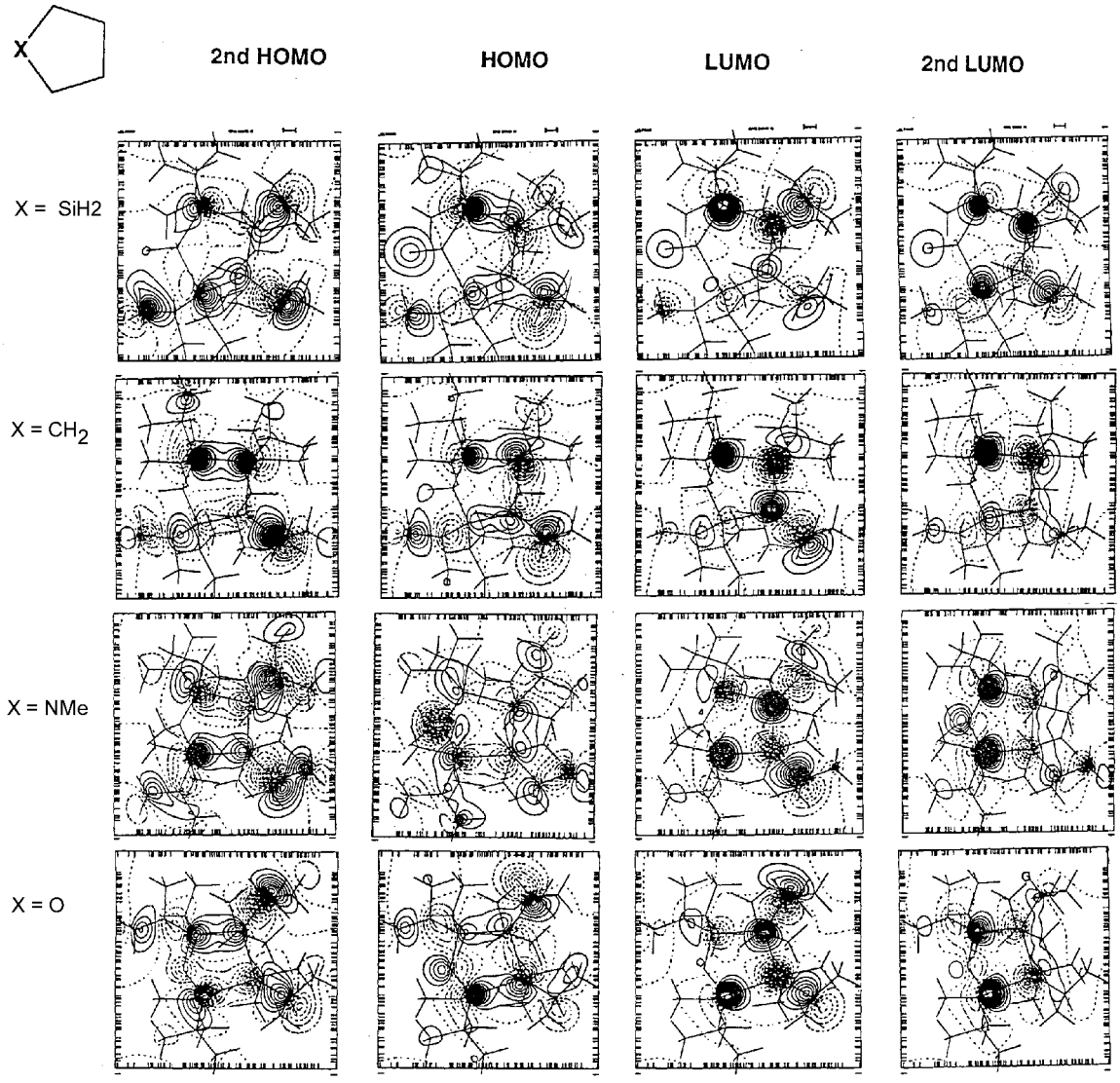

Figure 5. Orbital pictures of the frontier orbitals of $[(i\mathrm{Pr})_2\mathrm{Si}]_4\mathrm{X}$ (X = SiH_2, CH_2, NMe, and O)

Table 20. Frontier orbital levels [eV] of $[(i\mathrm{Pr})_2\mathrm{Si}]_n\mathrm{X}$ at PM3 level

ring size	n	X	compd	HOMO	LUMO	E_T[a]
4	3	CH_2	**1a**	-8.00	-1.29	6.71
		NMe	"	-7.97	-1.20	6.77
		N(*i*Pr)[b]	"	-7.95	-1.22	6.73
		O	**5a**	-7.84	-1.18	6.66
		SiH_2	"	-8.55	-1.58	6.97
5	4	CH_2	**2a**	-8.39	-1.19	7.20
		NMe	"	-8.01	-1.48	6.53
		N(*i*Pr)[b]	"	-7.76	-1.41	6.35
		O	**6a**	-7.79	-1.48	6.31
		SiH_2	"	-8.50	-1.69	6.81

[a] Transition energy. [b] For convenience, the bulkiness of the two β-carbon atoms of the isopropyl group is assumed to be close to that of the cyclohexyl group; polar substituent constant $\sigma^*(i\mathrm{Pr}) = -0.190$, $\sigma^*(C_6H_{11}) = -0.15$ (see ref.[17]).

It seemed quite interesting to compare the theoretical prediction with experimental results obtained by photochemical cleavage of the heteroatom-containing silacycles Si_nX (n = 3, 4; X = CH_2, NC_6H_{11}, O).[8,37] We therefore investigated photochemical decomposition of the series of silacycles in a hydrocarbon solvent at room temperature or at 77 K under various reaction conditions in the absence or presence of reactants to trap reactive intermediates produced during the reactions.[1b] With a low-pressure mercury lamp (λ = 254 nm light)[8,37a] or a halogen lamp (λ > 390 nm light) in the presence of a photosensitizer such as 9,10-dicyanoanthracene,[37b] various photochemical decompositions were carried out to give the corresponding products, which were characterized, identified, and quantitatively analyzed (**1**, **3**, **5**, **7**, **8**, **9**, **10**, and final products). The results, summarized in Scheme 4, clearly show that the bond scissions occurred exclusively at the Si−Si bonds, and not at the Si−X bonds, which indicated good agreements with the above predictions. Finally, it should be noted that the strain energies in the series of silacycles Si_nX (n = 3, 4; X = CH_2, NR^3, O, GeR'_2) probably affect the differences between their reaction rates, as has been previously shown for thermal reactions of homosilacycles.[1b,38]

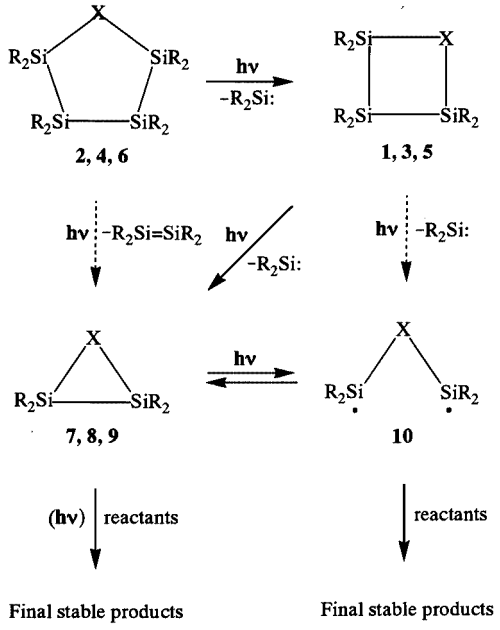

Scheme 4. Photochemical decompositions of heteroatom-containing silacycles Si_nX (n = 3, 4; X = CH_2, NR^3, and O) to give products; the paths shown with a dotted arrow do not seem to exist

Experimental Section

General Procedure: All reactions were carried out in dry flasks under an inert gas (N_2 or Ar). A commercially available 30% lithium dispersion in mineral oil was employed and was usually washed with the same solvent as used in subsequent reactions unless otherwise noted. In all preparations, the progress of the reaction in each step was monitored by GLC analysis. All melting points (uncorrected) were determined in sealed tubes, and for high melting point measurements a block heating apparatus equipped with a microscope were used. ^{1}H NMR spectra were recorded with Varian EM 360 A (60 MHz) (for **3b** and **5**), Hitachi 90H (90 MHz) and Varian Gemini 200M (200 MHz) spectrometers (for **1**, **2**, **3a**, **3c**, **3d**, **4**, and **6**) in $CDCl_3$ or C_6D_6 with Me_4Si as an internal standard. ^{13}C NMR spectra were recorded with Hitachi 90H (for **3a**, **3b**, **5**, and **6**) and Varian Gemini 200M (for **1**, **2**, **3c**, **3d**, and **4**) spectrometers in $CDCl_3$ or C_6D_6 with Me_4Si as an internal standard. For convenience, some spectroscopic data signals include the multiplicities in parentheses determined by the off-resonance technique. ^{29}Si NMR spectra were recorded in $CDCl_3$ or C_6D_6 with Hitachi 90H (for **3**−**6**) and JEOL ALPHA 500 (for **1** and **2**) spectrometers. Mass spectra were recorded with a JEOL DX 302 spectrometer (Ip = 30 or 70 eV). UV spectra were obtained with a Hitachi 200-10 spectrometer. GLC analysis was performed with an Ohkura GC-103 gas chromatograph equipped with a glass column (1 m) packed with SE-30 (10%) on Celite 545-AW (60−80 mesh). Cyclic voltammetry was performed with a Hokuto Denko Model HB-107A function generator and a Hokuto Denko Model HA-101 potentiostat. A cyclic voltammogram obtained at a scan rate of 250 mV/s was recorded with a Rikadenki X-Y recorder Model BW 133. For high-speed recording, a two-channel wave memory (NF Model MW-812A) was employed.

Materials: Tetrahydrofuran and benzene used in synthesis were dried with sodium wire and then freshly distilled out from a flask containing benzophenone/ketyl radical before use. Hexane, cyclohexane, and pentane were dried with lithium aluminum hydride and freshly distilled before use. Butyllithium solution in pentane (ca. 1.78 M) was commercially available. Spectrochemical grade cyclohexane was used for the determination of UV spectra. For cyclic voltammetry, spectrochemical grade acetonitrile and dichloromethane were dried by heating under reflux with P_2O_5 and freshly distilled under nitrogen before use. Other solvents and materials were commercially available.

Synthesis of *C*-Substituted Compounds 1 and 2: Compounds **1** and **2** were synthesized by reductive coupling of the corresponding α,ω-dichlorocarbosilanes with lithium as shown in Scheme 2, (a).

Synthesis of 2,2,3,3,4,4-Hexaisopropyl-2,3,4-trisilacyclobutane (1a): Typically, a solution of 1,4-dichloro-1,1,2,2,4,4-hexaisopropyl-1,2,4-trisilabutane $Cl(R_2Si)_2CH_2SiR_2Cl$ (R = *i*Pr) (**1a-1**, 0.161 g, 0.38 mmol) in a solvent mixture of THF (1.9 mL) and hexane (10.1 mL) was slowly added over 8 min at room temperature with stirring to a green suspension of lithium (69 mg, 2.98 mmol) and biphenyl (23 mg, 0.15 mmol) in THF (3.8 mL). After 2 h of stirring and addition of hexane, the unchanged lithium was filtered off. Purification by short column chromatography (silica gel, hexane) gave **1a** (0.134 g, 93% purity by GLC) as a colorless liquid, which was isolated by preparative GLC. ^{1}H NMR ($CDCl_3$): δ = 0.03 (s, 2 H, $C_{(ring)}H_2$), 1.09−1.12 [m, 24 H, $Si^{\alpha}CH(CH_3)_2$], 1.24 [d, 12 H, $Si^{\beta}CH(CH_3)_2$], 1.13−1.20 (m, 4 H, $Si^{\alpha}CHMe_2$), 1.41−1.50 (m, 2 H, $Si^{\beta}CHMe_2$). ^{13}C NMR ($CDCl_3$) −4.0 ($C_{(ring)}H_2$), 13.6 ($Si^{\beta}CHMe_2$), 14.9 ($Si^{\alpha}CHMe_2$), 19.7 and 20.0 [$Si^{\alpha}CH(CH_3)_2$], 22.5 [$Si^{\beta}CH(CH_3)_2$]. MS: m/z (%) = 356 (100) [M^+], 313 (60) [M − (*i*Pr)]$^+$, 271 (80) [M − (*i*Pr) − C_3H_6]$^+$. $C_{19}H_{44}Si_3$: calcd. C 63.96, H 12.43; found C 64.18, H 12.63. The above 1,4-dichlorotrisilabutane (**1a-1**) was prepared by a method similar to that used for the preparation of the methyl analogue $Br(Me_2Si)_2CH_2SiMe_2Br$,[3a] starting from R_2SiHCl (R = *i*Pr) via HR_2SiCH_2Cl (GLC yield, 36%), $HR_2SiCH_2SiR_2Ph$ (74%), $ClR_2SiCH_2SiR_2Ph$ (100%), $PhR_2SiSiR_2CH_2SiR_2Ph$ (100%), and then $ClR_2SiSiR_2CH_2SiR_2Cl$ (**1a-1**) (70%) (overall yield based on R_2SiHCl used, 19%); Colorless liquid; b.p. 103−105 °C/0.2 Torr. ^{1}H NMR ($CDCl_3$): δ = 0.28 (s, 2 H, $SiCH_2Si$), 1.11−1.50 [m, 42 H, $SiCH(CH_3)_2$]. ^{13}C NMR ($CDCl_3$): δ = 7.6 ($SiCH_2Si$), 13.5 (Si^2CHMe_2), 16.5 (Si^1CHMe_2), 17.0 (Si^4CHMe_2), 17.7 [$Si^2CH(CH_3)_2$], 18.1 and 18.6 [$Si^1CH(CH_3)_2$], 19.6 [$Si^4CH(CH_3)_2$]. MS: m/z (%) = 383 (5) [M − (*i*Pr)]$^+$, 341 (3) [M − (*i*Pr) − C_3H_6]$^+$, 274 (100) [M − $(iPr)_2SiCl$]$^+$. $C_{19}H_{44}Cl_2Si_3$: calcd. C 53.35, H 10.37; found C 53.27, H 10.36.

Synthesis of 2,2,3,3,4,4-Hexaneopentyl-2,3,4-trisilacyclobutane (1b): This compound was synthesized by a method similar to that used for **1a**, by treatment of 1,4-dichloro-1,1,2,2,4,4-hexaneopentyl-1,2,4-trisilabutane $Cl(R_2Si)_2CH_2SiR_2Cl$ (**1b-1**: R = $tBuCH_2$; 0.599 g, 1.00 mmol, THF 5 mL/hexane 15 mL) with lithium (0.220 g, 9.5 mmol) and biphenyl (33 mg, 0.21 mmol, THF 10 mL) for 2.5 h. Compound **1b** (recrystallized from ethanol/pentane): 0.379 g, 72% yield; m.p. 138−140 °C. ^{1}H NMR ($CDCl_3$): δ = 0.44 (s, 2 H, $C_{(ring)}H_2$), 1.05 [s, 18 H, $Si^{\beta}CH_2C(CH_3)_3$], 1.06 [s, 36 H, $Si^{\alpha}CH_2C(CH_3)_3$], 1.15−1.19 [m, 12 H, $SiCH_2(tBu)$]. ^{13}C NMR ($CDCl_3$) δ = −6.7 ($C_{(ring)}H_2$), 29.5 [$Si^{\beta}CH_2(tBu)$], 31.4 ($Si^{\beta}CH_2CMe_3$), 32.0 ($Si^{\alpha}CH_2CMe_3$), 33.6 [$Si^{\alpha}CH_2(tBu)$], 33.8 [$Si^{\alpha}CH_2C(CH_3)_3$], 33.9 [$Si^{\beta}CH_2C(CH_3)_3$]. MS: m/z (%) = 524 (28) [M^+], 453 (45) [M − ($tBuCH_2$)]$^+$, 397 (13) [M − ($tBuCH_2$) − C_4H_8]$^+$, 341 (10) [M − ($tBuCH_2$) − $(C_4H_8)_2$]$^+$. $C_{31}H_{68}Si_3$: calcd. C 70.90, H 13.10; found C 70.52, H 13.05. The above 1,4-dichlorotrisilabutane (**1b-1**) was prepared by a method similar to that used for **1a-1**, starting from $R_2SiPhCl$ (R = $tBuCH_2$) via PhR_2SiCH_2Cl (GLC yield, 86%), $PhR_2SiCH_2SiR_2Ph$ (61%), $ClR_2SiCH_2SiR_2Cl$ (78%), $PhR_2SiSiR_2CH_2SiR_2Cl$ (100%), and then $ClR_2SiSiR_2CH_2SiR_2Cl$ (**1b**−**1**) (84%) (overall yield based on $R_2SiPhCl$ used, 34%);

m.p. 55−57 °C. ^{1}H NMR ($CDCl_3$): δ = 0.50 (s, 2 H, SiCH_2Si), 1.06, 1.08 and 1.11 [54 H, $SiCH_2C(CH_3)_3$], 1.13−1.32 [m, 12 H, SiCH_2(*t*Bu)]. ^{13}C NMR ($CDCl_3$): δ = 4.8 (SiCH_2Si), 32.0, 34.4, and 37.3 [CH_2(*t*Bu)], 31.6, 31.7, and 32.0 (CH_2CMe_3), 33.2, 33.3, and 34.0 [$CH_2C(CH_3)_3$]. MS: *m*/*z* (%) = 523 (9) [M − (tBuCH$_2$)]$^+$, 389 (100) [M − (tBuCH$_2$)$_2$SiCl]$^+$, 333 (10) [M − (tBuCH$_2$)$_2$SiCl − C_4H_8]$^+$. $C_{31}H_{68}Cl_2Si_3$: calcd. C 62.47, H 11.50; found C 62.20, H 11.42.

Synthesis of 2,2,3,3,4,4,5,5-Octaisopropyl-2,3,4,5-tetrasilacyclopentane (2a): This compound was synthesized by a similar method to that used for **1a**, by treatment of 1,5-dichloro-1,1,2,2,4,4,5,5-octaisopropyl-1,2,4,5-tetrasilapentane $Cl(R_2Si)_2CH_2(SiR_2)_2Cl$ (**2a−1**: R = *i*Pr; 0.175 g, 0.32 mmol, THF 6 mL/hexane 5 mL) with lithium (0.127 g, 5.5 mmol) and biphenyl (42 mg, 0.28 mmol) in THF (3.5 mL) for 30 min. Compound **2a** (recrystallized from ethanol): 0.130 g, 87% yield; m.p. 249 −263 °C. ^{1}H NMR ($CDCl_3$): δ = −0.09 (s, 2 H, $C_{(ring)}H_2$), 1.14 [d, 24 H, Si$^\alpha$CH(CH_3)$_2$], 1.21−1.26 [m, 28 H, Si$^\alpha$C*H*Me$_2$ and Si$^\beta$CH(CH_3)$_2$], 1.41−1.56 (m, 4 H, Si$^\beta$C*H*Me$_2$). ^{13}C NMR ($CDCl_3$) δ = −5.9 ($C_{(ring)}$H$_2$), 13.6 (Si$^\beta$*C*HMe$_2$), 15.3 (Si$^\alpha$*C*HMe$_2$), 20.3 and 20.4 [Si$^\alpha$CH(*C*H$_3$)$_2$], 22.5 and 22.8 [Si$^\beta$CH(*C*H$_3$)$_2$]. MS: *m*/*z* (%) = 470 (20) [M$^+$], 427 (100) [M − (*i*Pr)]$^+$, 385 (35) [M − (*i*Pr) − C_3H_6]$^+$. $C_{25}H_{58}Si_4$: calcd. C 63.74, H 12.41; found C 63.79, H 12.25. The 1,5-dichlorotetrasilapentane (**2a-1**) mentioned above was prepared by HCl bubbling in the presence of $AlCl_3$ catalyst (2.33 mmol) in benzene (17 mL), by chlorination of $Ph(R_2Si)_2CH_2(SiR_2)Cl$ (R = *i*Pr; 2.27 mmol), which was obtained in quantitative yield by treatment of **1a-1** (2.27 mmol in 7 mL of THF) with PhR_2SiLi (R = *i*Pr; 3.76 mmol in 4 mL of THF). Compound **2a-1**: 1.27 g, purity 86%; yield 89%; Preparative GLC separation gave analytical samples; viscous liquid. ^{1}H NMR ($CDCl_3$): δ = 0.25 (s, 2 H, SiCH_2Si), 1.1−1.4 [m, 56 H, Si*C*H(CH_3)$_2$]. ^{13}C NMR ($CDCl_3$) δ = −7.9 (Si*C*H$_2$Si), 14.5 (CH$_2$Si*C*HMe$_2$), 17.2 (ClSi*C*HMe$_2$), 18.3 and 18.8 [CH$_2$SiCH(*C*H$_3$)$_2$], 19.8 and 20.2 [ClSiCH(*C*H$_3$)$_2$]. MS: *m*/*z* (%) = 391 (100) [M − (*i*Pr$_2$SiCl)]$^+$, 349 (40) [M − (*i*Pr$_2$SiCl)− C_3H_6]$^+$. $C_{25}H_{58}Cl_2Si_4$: calcd. C 55.40, H 10.79; found C 54.97, H 10.80.

Synthesis of 2,2,3,3,4,4,5,5-Octaneopentyl-2,3,4,5-tetrasilacyclopentane (2b): This compound was synthesized by a method similar to that used for **1a**, by treatment of 1,5-dichloro-1,1,2,2,4,4,5,5-octaneopentyl-1,2,4,5-tetrasilapentane $Cl(R_2Si)_2CH_2(SiR_2)_2Cl$ (**2b−1**: R = tBuCH$_2$; 0.153 g, 0.20 mmol, THF 1 mL/hexane 3 mL) with lithium (44 mg, 1.9 mmol) and biphenyl (7 mg, 0.047 mmol) in THF (2 mL) for 1.5 h. Compound **2b** (recrystallized from ethanol): 0.107 g, 77% yield; m.p. 354−364 °C. ^{1}H NMR ($CDCl_3$): δ = 0.47 (s, 2 H, $C_{(ring)}H_2$), 1.07 [s, 36 H, Si$^\beta$CH$_2$C(CH_3)$_3$], 1.08 [s, 36 H, Si$^\alpha$CH$_2$C(CH_3)$_3$], 1.14−1.36 [m, 16 H, SiCH_2(*t*Bu)]. ^{13}C NMR ($CDCl_3$): δ = 1.5 ($C_{(ring)}$H$_2$), 30.1 [Si$^\beta$*C*H$_2$(*t*Bu)], 32.3 (Si$^\beta$CH$_2$*C*Me$_3$), 32.6 (Si$^\alpha$CH$_2$*C*Me$_3$), 33.1 [Si$^\alpha$*C*H$_2$(*t*Bu)], 34.1 [Si$^\alpha$CH$_2$C(*C*H$_3$)$_3$], 34.5 [Si$^\beta$CH$_2$C(*C*H$_3$)$_3$]. MS: *m*/*z* (%) = 694 (31) [M$^+$], 623 (21) [M − (tBuCH$_2$)]$^+$, 453 (13) [M − (tBuCH$_2$)$_3$Si]$^+$. $C_{41}H_{90}Si_4$: calcd. C 70.81, H 13.04; found C 70.40, H 12.94. The 1,5-dichlorotetrasilapentane (**2b-1**) mentioned above was prepared by a method similar to that used for **2a-1**, from $Ph(R_2Si)_2CH_2(SiR_2)_2Cl$ (R = tBuCH$_2$; 0.74 mmol), $AlCl_3$ catalyst (1.23 mmol in 6 mL of benzene), and HCl gas, as a crude product, 0.820 g (purity 63% by GLC; yield 91%). Recrystallization from hexane afforded analytical samples; m.p. 128−129 °C. ^{1}H NMR ($CDCl_3$): δ = 0.31 (s, 2 H, SiCH_2Si), 1.07 and 1.12 [72 H, SiCH$_2$C(CH_3)$_3$], 1.14−1.49 [m, 16 H, SiCH_2(*t*Bu)]. ^{13}C NMR ($CDCl_3$): δ = 2.9 (Si*C*H$_2$Si), 33.0 and 34.2 [*C*H$_2$(*t*Bu)], 31.7 and 32.8 (CH$_2$*C*Me$_3$), 33.4 and 34.1 [CH$_2$C(*C*H$_3$)$_3$]. MS: *m*/*z* (%) = 693 (6) [M − (tBuCH$_2$)]$^+$, 559 (100) [M − (tBuCH$_2$)$_2$SiCl]$^+$. $C_{41}H_{90}Cl_2Si_4$: calcd. C 64.25, H 11.84; found C 64.16, H 11.79.

Synthesis of *N*-Substituted Compounds 3 and 4: Compounds **3** and **4** were synthesized by treatment of the corresponding α,ω-dichlorosilanes with lithium alkylamide as shown in Scheme 2, (b) or (c).

Synthesis of 1-Cyclohexyl-2,2,3,3,4,4-hexaisopropyl-1-aza-2,3,4-trisilacyclobutane (3a) [Scheme 2, (b)]**:** Typically, a pentane solution of butyllithium (1.59 mL, 2.83 mmol) was added dropwise to a solution of cyclohexylamine (0.25 mL, 2.18 mmol) in THF (11 mL) at −75 to −60 °C. With stirring at the same temperature, the reaction progress was monitored by GLC for the peak intensity of the amine. When the intensity had decreased to a minimum, a solution of 1,3-dichloro-hexaisopropyltrisilane[5a] (0.50 g, 1.21 mmol) in THF (1 mL) was added to the reaction mixture at the same temperature. After additional stirring for 1 h at that temperature, 1 h at room temperature, and then heating under reflux for 10 h, the solvents were evaporated to give a solid, to which cyclohexane was added. After filtration, the resulting solution was concentrated, treated with water, and extracted with cyclohexane. The extracts were dried with calcium chloride, filtered, and concentrated to give a solid product, which was recrystallized from ethanol to afford colorless crystals of **3a** (0.36 g, 57% based on the dichlorotrisilane used); m.p. 208−213 °C. ^{1}H NMR ($CDCl_3$): δ = 1.08−1.15 [m, 24 H, Si$^\alpha$CH(CH_3)$_2$], 1.29−1.32 [m, 12 H, Si$^\beta$CH(CH_3)$_2$], 1.50−1.77 (m, 6 H, Si*C*HMe$_2$), 0.7−2.0 (m, 10 H, C$^{2-5}H_2$ in C_6H_{11}), 2.7−2.9 (m, 1 H, C^1H in C_6H_{11}). ^{13}C NMR ($CDCl_3$): δ = 14.8 (d, Si$^\beta$*C*HMe$_2$), 17.0 (d, Si$^\alpha$*C*HMe$_2$), 19.2 [q, Si$^\alpha$CH(*C*H$_3$)$_2$], 19.8 [q, Si$^\alpha$CH(*C*H$_3$)$_2$], 23.3 [q, Si$^\beta$CH(*C*H$_3$)$_2$]; 25.9 (t, C^4 in C_6H_{11}), 26.7 (t, C^{3,5} in C_6H_{11}), 37.8 (t, C^{2,6} in C_6H_{11}), 57.6 (d, C^1 in C_6H_{11}). MS: *m*/*z* (%) = 439 (8) [M$^+$], 396 (100) [M − (*i*Pr)]$^+$, 354 (7) [M − (*i*Pr) − C_3H_6]$^+$. $C_{24}H_{53}NSi_3$: calcd. C 65.52, H 12.14; found C 64.95, H 11.97.

Synthesis of 1-Cyclohexyl-2,2,3,3,4,4-hexaneopentyl-1-aza-2,3,4-trisilacyclobutane (3b): This compound was synthesized by a method similar to that used for **3a**, by treatment of 1,3-dichloro-1,1,2,2,3,3-hexaneopentyltrisilane $Cl(R_2Si)_3Cl$ (R = tBuCH$_2$; 2.00 g, 3.44 mmol)[10] with lithium cyclohexylamide (twice), prepared from cyclohexylamine (0.79 mL, 6.88 mmol in 20 mL of THF) and butyllithium (6.2 mL, 11.25 mmol in pentane). Compound **3b** (recrystallized from ethanol): 1.43 g, 69% yield; m.p. 228−238 °C. ^{1}H NMR ($CDCl_3$): δ = 1.08 [s, 36 H, Si$^\alpha$CH$_2$C(CH_3)$_3$], 1.11 [s, 18 H, Si$^\beta$CH$_2$C(CH_3)$_3$], 1.22 [broad s, 8 H, Si$^\alpha$CH_2(*t*Bu)], 1.32 [broad s, 4 H, Si$^\beta$CH_2(*t*Bu)], 1.0−1.9 (m, 10 H, C$^{2-5}H_2$ in C_6H_{11}), 2.5−2.9 (m, 1 H, C^1H in C_6H_{11}). ^{13}C NMR ($CDCl_3$): δ = 31.2 [t, Si$^\beta$*C*H$_2$(*t*Bu)], 31.4 (s, Si$^\alpha$CH$_2$*C*Me$_3$), 33.4 (s, Si$^\beta$CH$_2$*C*Me$_3$), 33.9 [q, Si$^\alpha$CH$_2$C(*C*H$_3$)$_3$], 34.2 [q, Si$^\beta$CH$_2$C(*C*H$_3$)$_3$], 37.5 [t, Si$^\alpha$*C*H$_2$(*t*Bu)], 26.8 (t, C^4 in C_6H_{11}), 28.7 (t, C^{3,5} in C_6H_{11}), 37.8 (t, C^{2,6} in C_6H_{11}), 59.2 (d, C^1 in C_6H_{11}). MS: *m*/*z* (%) = 607 (60) [M$^+$], 536 (100) [M − (tBuCH$_2$)]$^+$, 436 (45) [M − (tBuCH$_2$)$_2$SiH]$^+$, 365 (45) [M − (tBuCH$_2$)$_3$SiH]$^+$. $C_{36}H_{77}NSi_3$: calcd. C 71.09, H 12.76; found C 71.13, H 12.62.

Synthesis of 1-Cyclohexyl-3-isopropyl-2,2,3,4,4-pentaneopentyl-1-aza-2,3,4-trisilacyclobutane (3c): This compound was synthesized by a method similar to that used for **3a**, by treatment of 1,3-dichloro-2-isopropyl-1,1,2,3,3-pentaneopentyltrisilane $ClSiR_2$-$SiRR'SiR_2Cl$ (**3c-1**: R = tBuCH$_2$, R′ = *i*Pr; 0.679 g, 1.23 mmol) with lithium cyclohexylamide (twice), prepared from cyclohexylamine (0.278 mL, 2.46 mmol in 15 mL of THF) and butyllithium (2.2 mL, 3.20 mmol in pentane). Compound **3c** (recrystallized from ethanol): 0.386 g, 54% yield; m.p. 219−225 °C. ^{1}H NMR ($CDCl_3$): δ = 1.03 [s, 2 H, Si$^\beta$CH_2(*t*Bu)], 1.09 [s, 36 H, Si$^\alpha$CH$_2$C(CH_3)$_3$], 1.20−1.35 [m, 34 H, C*H*(CH_3)$_2$, Si$^\alpha$CH_2(*t*Bu), Si$^\beta$CH$_2$C(CH_3)$_3$, C$^{2-6}H_2$ in C_6H_{11}], 2.7−2.9 (m, 1 H, C^1H in C_6H_{11}). ^{13}C NMR ($CDCl_3$): δ = 13.6 (Si*C*HMe$_2$), 21.2 [SiCH(*C*H$_3$)$_2$], 28.6

[$Si^{\beta}CH_2(tBu)$], 31.1 and 31.6 ($Si^{\alpha}CH_2CMe_3$), 31.9 ($Si^{\beta}CH_2CMe_3$), 33.7 [$Si^{\beta}CH_2C(CH_3)_3$], 34.2 [$Si^{\alpha}CH_2C(CH_3)_3$], 37.1 and 38.1 [$Si^{\alpha}CH_2(tBu)$], 26.1 (C^4 in C_6H_{11}), 26.9 ($C^{3,5}$ in C_6H_{11}), 39.7 ($C^{2,6}$ in C_6H_{11}), 59.5 (C^1 in C_6H_{11}). MS: *m/z* (%) = 579 (5) [M^+], 536 (3) [M − (*i*Pr)]$^+$, 508 (100) [M − (tBuCH$_2$)]$^+$. $C_{34}H_{73}NSi_3$: calcd. C 70.38, H 12.68; found C 69.90, H 12.69. The 1,3-dichlorotrisilane (**3c-1**) mentioned above was prepared by chlorination of the corresponding trisilane $HSiR_2SiRR'SiR_2H$ (**3c-2**; R = tBuCH$_2$, R′ = *i*Pr). Phosphorus pentachloride (0.37 g, 1.74 mmol) was added portionwise and slowly to a solution of **3c-2** (0.27 g, 0.56 mmol in 10 mL of benzene), and the mixture was stirred for ca. 18 h at room temperature. After evaporation of the solvent, hexane was added to the resulting mixture, which was then filtered. The filtrate, on evaporation of the solvents, gave **3c-1**, viscous liquid: 0.26 g, 0.83% yield. MS: *m/z* (%) = 552 (1) [M^+], 509 (1) [M − (*i*Pr)]$^+$, 481(100) [M − (tBuCH$_2$)]$^+$, 347 (100) [M − (tBuCH$_2$)$_2$SiCl]$^+$. The trisilane **3c-2** was prepared by lithium-mediated (0.46 g, 66 mmol in 50 mL of THF) cross-coupling with chlorodineopentylsilane (5.16 g, 25 mmol) and dichloro(isopropyl)(neopentyl)silane (2.37 g, 11 mmol) in THF (80 mL) (with magnetic stirring and ultrasound irradiation in a hot water bath). Compound **3c-2** (recrystallized from ethanol): 1.1 g, 20% yield; m.p. 57−58 °C. ^{1}H NMR (C_6D_6) δ = 1.13(s), 1.15(s), and 0.85−2.1(m) [62 H, $SiCH(CH_3)_2$, $SiCH(CH_3)_2$, $SiCH_2C(CH_3)_3$, $SiCH_2(tBu)$], 4.38 (m, 2 H, Si*H*). ^{13}C NMR (C_6D_6) δ = 13.6 ($SiCHMe_2$), 21.3 [$SiCH(CH_3)_2$], 29.0 [$Si^2CH_2(tBu)$], 30.1 ($Si^2CH_2CMe_3$), 30.7 [$Si^{1,3}CH_2(tBu)$], 31.6 ($Si^{1,3}CH_2CMe_3$), 32.9 [$Si^{1,3}CH_2C(CH_3)_3$], 33.8 [$Si^2CH_2C(CH_3)_3$]. MS: *m/z* (%) = 484 (7) [M^+], 441 (4) [M − (*i*Pr)]$^+$, 413 (10) [M − (tBuCH$_2$)]$^+$, 313 (100) [M − (tBuCH$_2$)$_2$SiH]$^+$. $C_{28}H_{64}Si_3$: calcd. C 69.33, H 13.30; found C 69.01, H 13.32.

Synthesis of 1-Cyclohexyl-3,3-diisopropyl-2,2,4,4-tetraneopentyl-1-aza-2,3,4-trisilacyclobutane (3d): This compound was synthesized by a method similar to that used for **3a**, by treatment of 1,3-dichloro-2,2-diisopropyl-1,1,3,3-tetraneopentyltrisilane $ClSiR_2SiR'_2SiR_2Cl$ (**3d-1**: R = tBuCH$_2$, R′ = *i*Pr; 0.55 g, 1.0 mmol) with lithium cyclohexylamide, prepared from cyclohexylamine (1.2 mL, 10.4 mmol in 7 mL of THF) and butyllithium (8.2 mL, 13.5 mmol in pentane). Compound **3d** (recrystallized from 2-propanol): 0.23 g, 42% yield; m.p. 291−297 °C. ^{1}H NMR ($CDCl_3$): δ = 1.09 [s, 36 H, $CH_2C(CH_3)_3$], 0.76−1.95 [m, 32 H, $CH(CH_3)_2$, $CH_2(tBu)$, $C^{2-6}H_2$ in C_6H_{11}], 2.70−2.85 (m, 1 H, C^1H in C_6H_{11}). ^{13}C NMR ($CDCl_3$): δ = 12.9 ($SiCHMe_2$), 21.6 [$SiCH(CH_3)_2$], 31.1 (CH_2CMe_3), 34.0 [$CH_2C(CH_3)_3$], 37.6 [$SiCH_2(tBu)$], 25.9 (C^4 in C_6H_{11}), 26.8 ($C^{3,5}$ in C_6H_{11}), 38.2 ($C^{2,6}$ in C_6H_{11}), 59.0 (C^1 in C_6H_{11}). MS: *m/z* (%) = 651 (10) [M^+], 508 (25) [M − (*i*Pr)]$^+$, 482 (100) [M − (tBuCH$_2$)]$^+$. $C_{32}H_{69}NSi_3$: calcd. C 69.61, H 12.60; found C 69.42, H 12.46. The 1,3-dichlorotrisilane (**3d-1**) mentioned above was prepared by chlorination of the corresponding trisilane $HSiR_2SiR'_2SiR_2H$ (**3d-2**: R = tBuCH$_2$, R′ = *i*Pr; 0.52 g, 1.13 mmol) with phosphorus pentachloride (1.67 g, 7.97 mmol) in benzene (7 mL). Compound **3d-1**: viscous liquid; 0.55 g, 92% yield. MS: *m/z* (%) = 481 (4) [M − (*i*Pr)]$^+$, 453 (20) [M − (tBuCH$_2$)]$^+$, 319 (100) [M − (tBuCH$_2$)$_2$SiCl]$^+$. The trisilane **3d-2** was prepared by lithium-mediated (0.62 g, 89 mmol in 13 mL of THF) cross-coupling with chlorodineopentylsilane (5.71 g, 28 mmol) and dichlorodiisopropylsilane (2.38 g, 13 mmol) in THF (15 mL). Compound **3d-2** (recrystallized from ethanol): 2.37 g, 40% yield; m.p. 67−68 °C. ^{1}H NMR ($CDCl_3$): δ = 1.02 [s, 36 H, $CH_2C(CH_3)_3$], 0.78−1.50 [m, 22 H, $CH(CH_3)_2$, $CH_2(tBu)$], 4.10−4.17 (m, 2 H, Si*H*). ^{13}C NMR ($CDCl_3$): δ = 14.7 ($CHMe_2$), 23.0 [$CH(CH_3)_2$], 31.8 [$CH_2(tBu)$], 33.2 (CH_2CMe_3), 34.5 [$CH_2C(CH_3)_3$]. MS: *m/z* (%) = 456 (3) [M^+], 413 (6) [M − (*i*Pr)]$^+$, 385 (8) [M − (tBuCH$_2$)]$^+$, 285 (100) [M − (tBuCH$_2$)$_2$SiH]$^+$. $C_{26}H_{60}Si_3$: calcd. C 68.33, H 13.23; found C 68.39, H 13.39.

Synthesis of 1-Cyclohexyl-2,2,3,3,4,4,5,5-octaisopropyl-1-aza-2,3,4,5-tetrasilacyclopentane (4a): This compound was synthesized by a method similar to that used for **3a** [Scheme 2, (c)], by treatment of 1,4-dichloro-1,1,2,2,3,3,4,4-octaisopropylcyclotetrasilane[11] $Cl(R_2Si)_4Cl$ (R = *i*Pr; 1.4 g, 2.6 mmol) with lithium cyclohexylamide, prepared from cyclohexylamine (0.9 mL, 7.9 mmol in 5 mL of THF) and butyllithium (6.5 mL, 10.2 mmol in hexane). Compound **4a** (recrystallized from 2-propanol): 0.51 g, 35% yield; m.p. 346−350 °C. ^{1}H NMR (δ, C_6D_6) 1.22−1.34 [m, 24 H, $Si^{\alpha}CH(CH_3)_2$], 1.36−1.48 [m, 24 H, $Si^{\beta}CH(CH_3)_2$], 1.60−1.76 (m, 8 H, $SiCHMe_2$), 1.2−2.0 (m, 10 H, $C^{2-6}H_2$ in C_6H_{11}), 3.0−3.2 (m, 1 H, C^1H in C_6H_{11}). ^{13}C NMR (C_6D_6) δ = 15.2 ($Si^{\beta}CHMe_2$), 17.8 ($Si^{\alpha}CHMe_2$), 20.4 and 20.6 [$Si^{\alpha}CH(CH_3)_2$], 24.1 and 24.4 [$Si^{\beta}CH(CH_3)_2$]; 26.3 (C^4 in C_6H_{11}), 27.9 ($C^{3,5}$ in C_6H_{11}), 38.9 ($C^{2,6}$ in C_6H_{11}), 59.0 (C^1 in C_6H_{11}). MS: *m/z* (%) = 559 (7) [M^+], 510 (100) [M − (*i*Pr)]$^+$, 468 (20) [M − (*i*Pr) − C_3H_6]$^+$, 446 (20) [M − (*i*Pr) − (C_3H_6)$_2$]$^+$. $C_{30}H_{67}NSi_4$: calcd. C 65.01, H 12.19; found C 64.50, H 11.98.

Synthesis of 1-Cyclohexyl-2,2,3,3,4,4,5,5-octaneopentyl-1-aza-2,3,4,5-tetrasilacyclopentane (4b): This compound was synthesized by a method similar to that used for **3a**, by treatment of 1,4-dichloro-1,1,2,2,3,3,4,4-octaneopentyltetrasilane[11] $Cl(R_2Si)_4Cl$ (R = tBuCH$_2$; 0.58 g, 0.77 mmol) with lithium cyclohexylamide, prepared from cyclohexylamine (1.4 mL, 12.3 mmol in 3 mL of THF) and butyllithium (10.1 mL, 16.0 mmol in pentane). Compound **4b** (recrystallized from 2-propanol): 0.23 g, 38% yield; m.p. 379−383 °C. ^{1}H NMR ($CDCl_3$): δ = 1.12 (s), and 1.13 (s) [72 H, $SiCH_2C(CH_3)_3$], 0.7−1.0 (m), 1.15−1.30 (m), and 1.30−2.2 (m) [26 H, $C^{2-6}H_2$ in C_6H_{11}, $SiCH_2(tBu)_3$], 3.0−3.2 (m, 1 H, C^1H in C_6H_{11}). ^{13}C NMR ($CDCl_3$) (tentative) δ = 30.3 [t, $Si^{\beta}CH_2(tBu)$], 31.7 (s, $Si^{\beta}CH_2CMe_3$), 32.1 (s, $Si^{\alpha}CH_2CMe_3$), 34.4 [q, $Si^{\beta}CH_2C(CH_3)_3$], 34.5 [q, $Si^{\alpha}CH_2C(CH_3)_3$], 36.9 [t, $Si^{\alpha}CH_2(tBu)$], 26.0 (t, C^4 in C_6H_{11}), 27.1 (t, $C^{3,5}$ in C_6H_{11}), 37.8 (t, $C^{2,6}$ in C_6H_{11}), 59.5 (d, C^1 in C_6H_{11}). MS: *m/z* (%) = 777 (3) [M^+], 706 (100) [M − (tBuCH$_2$)]$^+$, 536 (30) [M − (tBuCH$_2$)$_3$Si]$^+$. $C_{46}H_{99}NSi_4$: calcd. C 70.78, H 12.82; found C 70.96, H 12.82.

Synthesis of 1-Cyclohexyl-3,3,4,4-tetraisopropyl-2,2,5,5-tetraneopentyl-1-aza-2,3,4,5-tetrasilacyclopentane (4c): This compound was synthesized by a method similar to that used for **3a**, by treatment of 1,4-dichloro-2,2,3,3-tetraisopropyl-1,1,4,4-tetraneopentyltetrasilane $ClSiR_2(SiR'_2)_2SiR_2Cl$ (**4c-1**: R = tBuCH$_2$, R′ = *i*Pr; 0.59 g, 0.90 mmol) with lithium cyclohexylamide, prepared from cyclohexylamine (3.46 mL, 28.7 mmol in 8 mL of THF) and butyllithium (17.1 mL, 27.9 mmol in pentane). Compound **4c** (recrystallized from 2-propanol): 0.28 g, 47% yield; m.p. 364−366 °C. ^{1}H NMR (C_6D_6) δ = 1.09 [s, 36 H, $CH_2C(CH_3)_3$], 0.78−2.10 [m, 51 H, $CH(CH_3)_2$, $CH_2(tBu)$, $C^{2-6}H_2$ in C_6H_{11}], 3.10−3.25 (m, 1 H, C^1H in C_6H_{11}). ^{13}C NMR ($CDCl_3$): δ = 14.5 ($SiCHMe_2$), 23.3 and 23.8 [$SiCH(CH_3)_2$], 31.7 (CH_2CMe_3), 34.1 [$CH_2C(CH_3)_3$], 36.7 [$CH_2(tBu)$], 26.0 (C^4 in C_6H_{11}), 27.0 ($C^{3,5}$ in C_6H_{11}), 37.6 ($C^{2,6}$ in C_6H_{11}), 60.0 (C^1 in C_6H_{11}). MS: *m/z* (%) = 665 (3) [M^+], 622 (10) [M − (*i*Pr)]$^+$, 594 (100) [M − (tBuCH$_2$)]$^+$. $C_{38}H_{83}NSi_4$: calcd. C 68.49, H 12.55; found C 68.49, H 12.46. The 1,4-dichlorotrisilane (**4c-1**) mentioned above was prepared by chlorination of the corresponding tetrasilane $HSiR_2(SiR'_2)_2SiR_2H$ (**4c-2**: R = tBuCH$_2$, R′ = *i*Pr; 1.00 g, 1.75 mmol) with phosphorus pentachloride (1.30, 6.19 mmol) in benzene (15 mL). Compound **4c-1** (recrystallized from hexane): 0.53 g, 47% yield; m.p. 65−66 °C. MS: *m/z* (%) 569 (10) [M − (tBuCH$_2$)]$^+$, 433 (100) [M − (tBuCH$_2$)$_2$SiCl]$^+$. The tetrasilane **4c-2** was prepared by lithium-mediated (1.51 g,

270 mmol in 80 mL of THF) cross-coupling with 1,2-dichlorotetraisopropyldisilane (7.36 g, 24.6 mmol) and chlorodineopentylsilane (14.24 g, 68.3 mmol) in THF (20 mL). Compound **4c-2** (recrystallized from pentane/ethanol): 10.6 g, 69% yield; m.p. 94−95 °C. ^{1}H NMR ($CDCl_3$): δ = 1.04 [s, 36 H, $CH_2C(CH_3)_3$], 0.82−1.50 [m, 36 H, $CH(CH_3)_2$, CH_2(*t*Bu)], 4.20−4.28 (m, 2 H, Si*H*). ^{13}C NMR ($CDCl_3$): δ = 13.9 (*C*HMe$_2$), 22.2 [$CH(CH_3)_2$], 29.8 (CH_2CMe_3), 31.5 [CH_2(*t*Bu)], 32.7 [$CH_2C(CH_3)_3$]. MS: *m*/*z* (%) = 570 (1) [M$^+$], 527 (10) [M − (*i*Pr)]$^+$, 499 (20) [M − (tBuCH$_2$)]$^+$, 399 (100) [M − (tBuCH$_2$)$_2$SiH]$^+$. $C_{32}H_{74}Si_4$: calcd. C 67.28, H 13.06; found C 67.06, H 13.07.

Synthesis of 1-Propyl-2,2,3,3,4,4,5,5-octaneopentyl-1-aza-2,3,4,5-tetrasilacyclopentane (4d): This compound was synthesized by a method similar to that used for **3a**, by treatment of 1,4-dichlorooctaneopentyltetrasilane[11] $Cl(R_2Si)_4Cl$ (R = tBuCH$_2$; 0.52 g, 0.69 mmol) with lithium propylamide, prepared from propylamine (0.44 g, 5.34 mmol in 3 mL of THF) and butyllithium (4.0 mL, 7.01 mmol in pentane). Compound **4d** (recrystallized from 2-propanol): 0.18 g, 35% yield; m.p. 396−399 °C. ^{1}H NMR ($CDCl_3$): δ = 0.83 (t, 3 H, $NCH_2CH_2CH_3$), 1.07 [s, 36 H, $Si^{\alpha}CH_2C(CH_3)_3$], 1.12 [s, 36 H, $Si^{\beta}CH_2C(CH_3)_3$], 1.17 (s), 1.24 (s), 1.31 (s), 1.38 (s), 1.43 (s), and 1.46−1.75 (m) [18 H, $NCH_2CH_2CH_3$, $Si^{\alpha}CH_2$(*t*Bu), $Si^{\beta}CH_2$(*t*Bu)], 2.90−3.10 (m, 2 H, $NCH_2CH_2CH_3$). ^{13}C NMR ($CDCl_3$): δ = 30.0 [$Si^{\beta}CH_2$(*t*Bu)], 31.6 ($Si^{\alpha}CH_2CMe_3$), 32.0 ($Si^{\beta}CH_2CMe_3$), 34.2 [$Si^{\beta}CH_2C(CH_3)_3$], 34.4 [$Si^{\alpha}CH_2C(CH_3)_3$], 36.5 [$Si^{\alpha}CH_2$(*t*Bu)], 11.7 (C^3 in C_3H_7), 27.8 (C^2 in C_3H_7), 51.6 (C^1 in C_3H_7). MS: *m*/*z* (%) = 737 (3) [M$^+$], 666 (100) [M − (tBuCH$_2$)]$^+$, 497 (15) [M − (tBuCH$_2$)$_4$Si$_2$]$^+$. $C_{43}H_{95}NSi_4$: calcd. C 69.93, H 12.96; found C 69.57, H 12.80.

Synthesis of *O*-Substituted Compounds 5 and 6: Compounds **5** and **6** were synthesized by treatment of the corresponding α-ω-dichlorosilanes with H_2O or NaOH as shown in Scheme 2, (d).

Synthesis of 2,2,3,3,4,4-Hexaisopropyl-1-oxa-2,3,4-trisilacyclobutane (5a): Typically, H_2O (1 mL, 56 mmol) was added at 53 °C with stirring to a solution of 1,3-dichlorohexaisopropyltrisilane[5a] (3.50 g, 8.5 mmol) in degassed triethylamine (20 mL). After the mixture had been stirred for 1 h at this temperature, degassed cyclohexane was added, and the mixture was extracted and dried with calcium chloride. After filtration, the filtrate was concentrated to give a solid product, which was recrystallized from methanol to afford colorless crystals of **5a** (see also ref.[8]) (0.85 g, 28%); m.p. 100−103 °C. ^{1}H NMR (C_6D_6) δ = 1.0−1.6 [m, 42 H, $SiCH(CH_3)_2$, $SiCH(CH_3)_2$]. ^{13}C NMR (C_6D_6) δ = 13.7 (d, $Si^{\beta}CHMe_2$), 16.6 (d, $Si^{\alpha}CHMe_2$), 17.9 [q, $Si^{\alpha}CH(CH_3)_2$], 22.7 [q, $Si^{\beta}CH(CH_3)_2$]. MS: *m*/*z* (%) = 358 (40) [M$^+$], 315 (100) [M − (*i*Pr)]$^+$, 273 (35) [M − (*i*Pr) − C_3H_6]$^+$. $C_{18}H_{42}OSi_3$: calcd. C 60.26, H 11.80; found C 59.58, H 11.72.

Synthesis of 2,2,3,3,4,4-Hexaneopentyl-1-oxa-2,3,4-trisilacyclobutane (5b): 1,3-Dichlorohexaneopentyltrisilane[10] $Cl(R_2Si)_3Cl$ (R = tBuCH$_2$; 0.59 g, 1.0 mmol in 10 mL of THF) was added to a mixture of NaOH (0.16 g, 4.0 mmol), THF (5 mL), and EtOH (5 mL). The mixture was stirred for 20 min at room temperature. After addition of hexane and filtration, the filtrate was concentrated and cyclohexane was then added. The solution was washed with dilute hydrochloric acid solution and water, dried, and then concentrated to give a crude product. Compound **5b** (recrystallized from ethanol/pentane) (see also ref.[8]): 0.41 g, 77% yield; m.p. 151−153 °C. ^{1}H NMR (C_6D_6) δ = 0.97 [s, 18 H, $Si^{\beta}CH_2C(CH_3)_3$], 1.03 [s, 36 H, $Si^{\alpha}CH_2C(CH_3)_3$], 1.22 [s, 4 H, $Si^{\beta}CH_2$(*t*Bu)], 1.28 [s, 8 H, $Si^{\alpha}CH_2$(*t*Bu)]. ^{13}C NMR ($CDCl_3$): δ = 29.0 [t, $Si^{\beta}CH_2$(*t*Bu)], 31.5 (s, $Si^{\alpha}CH_2CMe_3$), 31.8 (s, $Si^{\beta}CH_2CMe_3$), 33.7 [q, $Si^{\alpha}CH_2C(CH_3)_3$], 34.0 [q, $Si^{\beta}CH_2C(CH_3)_3$], 36.5 [t, $Si^{\alpha}CH_2$(*t*Bu)]. MS: *m*/*z* (%) = 526 (30) [M$^+$], 511 (25) [M − Me]$^+$, 455 (90) [M − (tBuCH$_2$)]$^+$, 399 (80) [M − (tBuCH$_2$) − C_4H_8]$^+$. $C_{30}H_{66}OSi_3$: calcd. C 68.36, H 12.62; found C 68.24, H 12.63.

Synthesis of 2,4-Diisopropyl-2,3,3,4-tetraneopentyl-1-oxa-2,3,4-trisilacyclobutane (5c): This compound was synthesized by a method similar to that used for **5a**, by hydrolysis of 1,3-dichloro-1,3-diisopropyltetraneopentyltrisilane $ClSiRR'SiR_2SiRR'Cl$ (**5c-1**: R = tBuCH$_2$, R′ = *i*Pr; 0.50 g, 0.95 mmol) with H_2O (1 mL) in triethylamine (15 mL), followed by workup of the resulting mixture. Compound **5c**: 0.39 g (purity: 92%) 87% yield, liquid; analytical samples were isolated by GLC purification. ^{1}H NMR (C_6D_6) δ = 1.05−1.30 (m) (composed of four peaks at 1.16, 1.19, 1.22, 1.25) [48 H, $SiCH(CH_3)_2$, $SiCH_2C(CH_3)_3$], 1.48 (broad s, 2 H, Si*C*HMe$_2$), 1.60 [broad s, 8 H, $SiCH_2$(*t*Bu)]. $C_{26}H_{58}OSi_3$: calcd. C 66.30, H 12.41; found C 66.10, H 12.42. The 1,3-dichlorotrisilane (**5c-1**) mentioned above was prepared by chlorination of the corresponding trisilane $HSiRR'SiR_2SiRR'H$ (**5c-2**: R = tBuCH$_2$, R′ = *i*Pr; 6.5 g, 14 mmol/CCl_4 30 mL) by chlorine gas bubbling. Compound **5c-1**: b.p. 185−195 °C/3 Torr; 3.8 g, 52% yield. ^{1}H NMR (C_6D_6) δ = 1.16 (s), and 1.18 (s) [48 H, $CH(CH_3)_2$, $CH_2C(CH_3)_3$], 1.35 [m, 4 H, $Si^{1,3}CH_2$(*t*Bu)], 1.50 [broad s, 4 H, Si^2CH_2(*t*Bu)], 1.73 (m, 2 H, *C*HMe$_2$). $C_{26}H_{58}Cl_2Si_3$: calcd. C 59.38, H 11.12; found C 59.41, H 11.15. The trisilane **5c-2** was prepared by lithium-mediated (fine cut, 0.4 g, 58 mmol in 40 mL of THF) cross-coupling with dichlorodineopentylsilane (2.4 g, 10.0 mmol) and chloro(isopropyl)-(neopentyl)silane (4.2 g, 23.6 mmol) in THF (15 mL). Compound **5c-2**: b.p. 124−127 °C/5 Torr; 1.8 g, 39% yield. ^{1}H NMR ($CDCl_3$):

Table 21. Crystal data, data collection, and refinement for four- and five-membered silacycles $[R_2Si]_nX$ (X = CH_2)

	Compd	
	1b	**2a**
	Crystal data	
formula	$C_{31}H_{68}Si_3$	$C_{25}H_{58}Si_4$
mol wt	525.135	471.075
crystal size/mm	0.3×0.1×0.1	0.3×0.2×0.2
cryst syst	Triclinic	Monoclinic
space group	$\bar{P}1$	$\bar{P}2_1/n$
a/Å	10.076(3)	20.860(3)
b/Å	11.900(4)	14.273(1)
c/Å	16.619(6)	10.487(1)
α/degree	102.04(2)	
β/degree	92.03(2)	95.36(2)
γ/degree	103.70(2)	
V/Å^3	1885(1)	3108.7(5)
Z	2	4
D_{calcd} (gcm^{-3})	0.924	1.006
	Data collection	
diffractmeter	Enraf-Nonius CAD4	Mac Science MXC18K
radiation (λ/Å)	1.5418(CuKα)	0.7107(MoKα)
temp/°C	23	23
scan mode	ω scan	ω scan
scan range (2θ)	4°∼120°	4°∼55°
no. of reflns collected	5986	7318
used (|Fo| ≧ |3σ|Fo|)	5617	7122
μ/cm^{-1}	12.45	2.0
abs cor method	ψ scan	no
transmission factor (min/max)	0.8235/0.9988	no
	Solution and refinement	
system used	UNICS III	Crystan
method	MULTAN 78	SIR 92
refinement method	full-matrix least squares	full-matrix least squares
R (Rw)	0.083(0.086)	0.061(0.083)
wrighting scheme	[a]	[b]
goodness of fit (S)	1.19	2.59
peaks in diff Fourier map (e/Å^3)	0.45/-0.52	0.53/-0.39

[a] $w = 1/\sigma^2 |F_o|$. [b] $w = 1/\sigma^2 |F_o|$.

δ = 0.61−1.96 (m), and 1.06 (m) [58 H, $CH(CH_3)_2$, $CH_2C(CH_3)_3$], 3.88 (m, 2 H, Si*H*). $C_{26}H_{60}Si_3$: calcd. C 68.33, H 13.23; found C 67.80, H 13.18.

Synthesis of 2,2,3,3,4,4,5,5-Octaisopropyl-1-oxa-2,3,4,5-tetrasilacyclopentane 6a: This compound was synthesized by a method similar to that used for **5b**, by hydrolysis of 1,4-dichlorooctaisopropyltetrasilane[11] $Cl(R_2Si)_4Cl$ (R = *i*Pr; 1.02 g, 1.9 mmol) with H_2O (3 mL) in THF (7 mL) at 50−60 °C for 15 h. Compound **6a** (recrystallized from methanol/ethanol): 0.88 g, 96% yield; m.p. 308−315 °C. ^{1}H NMR ($CDCl_3$): δ = 1.0−1.15 [m, 24 H, $Si^{\alpha}CH(CH_3)_2$], 1.20−1.35 [m, 24 H, $Si^{\beta}CH(CH_3)_2$], 1.35−1.56 (m, 8 H, $SiCHMe_2$). ^{13}C NMR ($CDCl_3$): δ = 13.4 (d, $Si^{\beta}CHMe_2$), 17.5 (d, $Si^{\alpha}CHMe_2$), 18.2 [q, $Si^{\alpha}CH(CH_3)_2$] and 18.8 [q, $Si^{\alpha}CH(CH_3)_2$], 22.6 [q, $Si^{\beta}CH(CH_3)_2$] and 22.9 [q, $Si^{\beta}CH(CH_3)_2$]. MS: *m*/*z* (%) = 472 (15) [M^+], 429 (100) $[M - (iPr)]^+$, 387 (50) $[M - (iPr) - C_3H_6]^+$, 345 (35) $[M - (iPr) - (C_3H_6)_2]^+$. $C_{24}H_{56}OSi_4$: calcd. C 60.29, H 11.90; found C 60.94, H 11.93.

Synthesis of 2,2,3,3,4,4,5,5-Octaneopentyl-1-oxa-2,3,4,5-tetrasilacyclopentane (6b): This compound was synthesized by a method similar to that used for **5a**, by treatment of 1,4-dichlorooctaneopentyltetrasilane[11] $Cl(R_2Si)_4Cl$ (R = $tBuCH_2$; 0.58 g, 0.77 mmol) with NaOH (ca. 1 mL of 1 M aq. solution) in THF (15 mL) at 50−60 °C for 20 h. Compound **6b** (recrystallized from hexane/ethanol): 0.5 g, 93% yield; m.p. 377−380 °C. ^{1}H NMR ($CDCl_3$): δ = 1.08 [s, 36 H, $Si^{\beta}CH_2C(CH_3)_3$], 1.10 [s, 36 H, $Si^{\alpha}CH_2C(CH_3)_3$], 1.16 [s, 8 H, $Si^{\beta}CH_2(tBu)$], 1.29 [s, 8 H, $Si^{\alpha}CH_2(tBu)$]. ^{13}C NMR ($CDCl_3$): δ = 29.6 [t, $Si^{\beta}CH_2(tBu)$], 31.8 (s, $Si^{\alpha}CH_2CMe_3$), 32.0 (s, $Si^{\beta}CH_2CMe_3$), 34.0 [q, $Si^{\alpha}CH_2C(CH_3)_3$], 34.3 [q, $Si^{\beta}CH_2C(CH_3)_3$], 36.0 [t, $Si^{\alpha}CH_2(tBu)$]. MS: *m*/*z* (%) = 696 (100) [M^+], 625 (65) $[M - (tBuCH_2)]^+$, 525 (50) $[M - (tBuCH_2)_3Si]^+$, 340 (70) $[(tBuCH_2)_4Si_2]^+$. $C_{40}H_{88}OSi_4$: calcd. C 68.88, H 12.72; found C 68.58, H 12.81.

Synthesis of Decaisopropylpentasilane E: This compound was synthesized (not optimized) by treatment of 1,4-dilithiooctaisopropyltetrasilane (in place of 1,4-dipotassiooctairopropyltetrasilane[14] with dichlorodiisopropylsilane [Scheme 2, (e)]. Freshly distilled anhydrous HMPA (1.1 mL) was added to a mixture of octaisopropylcyclotetrasilane **A** (168 mg, 0.368 mmol) and lithium (51 mg, 0.735 mmol). The mixture was stirred at room temperature for 2 h to afford a dark red-brown solution containing 1,4-dilithiooctaisopropyltetrasilane, to which benzene (5 mL) was then added. This solution, containing the 1,4-dilithiotetrasilane, was added dropwise by hypodermic syringe to a separate flask containing dichlorodiisopropylsilane (70 μL, 0.401 mmol) in benzene (2.5 mL) in an ice/water bath. After stirring at 0 °C for 30 min, the reaction mixture was mixed well with hexane (60 mL) and water (80 mL). After separation of the organic layer, it was washed well with water, dried with calcium chloride, and then filtered. The solution obtained was concentrated to give a solid product mixture, from which the reaction product, decaisopropylcyclopentasilane **E**, was isolated by repeated fractional recrystallization from a mixture of pentane/ethanol to afford 40 mg, 19% yield, m.p. 357−366 °C. It was found

Table 22. Crystal data, data collection, and refinement for four-membered silacycles $[R_2Si]_3X$ (X = NR_3)

	Compd			
	3a	**3b**	**3c**	**3d**
	Crystal data			
formula	$C_{24}H_{53}NSi_3$	$C_{36}H_{77}NSi_3$	$C_{34}H_{73}NSi_3$	$C_{32}H_{69}NSi_3$
mol wt	439.946	608.268	580.214	552.160
crystal size/mm	0.4×0.4×0.2	0.5×0.3×0.2	0.65×0.6×0.1	0.06×0.06×0.7
cryst syst	Monoclinic	Monoclinic	Monoclinic	Monoclinic
space group	$P2_1/n$	$P2_1/n$	$P2_1/n$	$P2_1/n$
a/Å	8.563(2)	19.505(5)	18.108(7)	10.732(4)
b/Å	18.828(3)	11.709(1)	12.104(1)	10.947(4)
c/Å	17.978(3)	20.858(6)	19.458(6)	31.78(1)
α/degree				
β/degree	101.79(3)	117.80(1)	110.54(2)	92.29(2)
γ/degree				
V/Å^3	2837.2(2)	4212.6(2)	3994.0(2)	3729(2)
Z	2	4	4	4
D_{calcd} (gcm^{-3})	1.030	0.96	0.97	0.98
	Data collection			
diffractmeter	Rigaku AFC-4	Enraf-Nonius CAD4	Enrauf-Nonius CAD4	Enrauf-Nonius CAD4
radiation (λ/Å)	0.7107(MoKα)	0.7107(MoKα)	0.7107(MoKα)	1.5418(CuKα)
temp/°C	23	23	23	23
scan mode	2θ/ω	ω scan	2θ/ω	2θ/ω
scan range (2θ)	4°∼55°	4°∼55°	4°∼55°	4°∼55°
no. of reflns				
collected	6646	10588	10234	6037
used (|Fo| ≧ 3σ |Fo|)	2855	5945	6890	3782
μ/cm^{-1}	1.64	1.34	1.40	12.486
abs cor method	no	no	ψ scan	ψ scan
transmission factor (min/max)	no	no	0.9650/0.999	0.85/1.00
	Solution and refinement			
system used	MULTAN 78 UNICS III	MULTAN 78 UNICS III	UNICS III MULTAN 78	UNICS III MULTAN 78
method				
refinement method	full-matrix least squares	full-matrix least squares	full-matrix least squares	full-matrix least squares
R (Rw)	0.063(0.070)	0.079(0.082)	0.060(0.060)	0.095(0.099)
wrighting scheme	[a]	[b]	[c]	[d]
goodness of fit (S)	2.04	2.03	1.31	2.64
peaks in diff Fourier map (e/Å^3)	0.35/-0.31	0.51/-0.34	0.38/-0.31	0.64/-0.36

[a] $w = 1/[84.2\cdot(\sin\theta/\lambda)^2 - 51.4\cdot(\sin\theta/\lambda) + 8.9]$. [b] $w = 1/(0.0078\cdot|F_o|^2 - 0.432\cdot|F_o| + 7.88)$. [c] $w = 1/(0.0078\cdot|F_o|^2 - 0.06402\cdot|F_o| + 1.54216)$. [d] $w = 1/(0.00788\cdot|F_o|^2 - 0.21670\cdot|F_o| + 6.00345)$.

that crystalline materials obtained from the filtrates contained the product **E** (ca. 20 mg, calculated), the unchanged starting compound (**A**), and a small amount of unidentified material. Compound **E** (see also ref.[14]): ^{1}H NMR ($CDCl_3$): δ = 1.33 [d, 60 H, $SiCH(CH_3)_2$], 1.43−1.62 (m, 10 H, $SiCHMe_2$). ^{13}C NMR ($CDCl_3$): δ = 15.9 ($SiCHMe_2$), 23.8 [$SiCH(CH_3)_2$]. MS: *m/z* (%) = 570 (5) [M^+], 527 (100) $[M - iPr]^+$, 485 (15) $[M - iPr - C_3H_6]^+$, 413 (10) $[M - iPr - 2(C_3H_6)]^+$. $C_{30}H_{70}Si_5$: calcd. C 62.25, H 12.45; found C 63.07, H 12.35.

Oxidation Potentials: Measurements of the oxidation potentials[7h,41] for **1**−**6** (10^{-3} M) by cyclic voltammetry were performed under N_2 (purified) in an anhydrous solvent (MeCN or CH_2Cl_2) containing Bu_4NClO_4 (TBAP, 0.1 M) as supporting electrolyte with a specially devised cell equipped with a working electrode (Pt inlay type, Beckmann 32273), counterelectrode (Pt wire), and saturated calomel electrode as a reference, connected to the cell through two salt bridges (saturated KCl solution), and the acetonitrile or dichloromethane solution of the sample. All runs were made at room temperature after a 15 min purge with N_2 and within 30 min of preparing the solution, experimental error ±0.02 V. All the results are summarized in Tables 18 and 19, together with those for the related compounds **A**−**D**, **F**−**I**.

Methods of Theoretical Calculations for Geometries, Frontier Molecular Orbitals, and Ring Strain Energies: Geometries of all molecules considered here were fully optimized at the PM3 level with the Gaussian 98 program.[42] They were then characterized as minima or transition states by calculation and diagonalization of the Hessian matrix of energy second derivatives at the same level of theory. The orbital pictures were drawn with the Gamess program.[43] The optimized structures for all four-membered rings are found to have C_s symmetry with a σ plane involving one silicon atom and heteroatom, except for X = N(*i*Pr) which is in a C_1 conformation. On the other hand, none of the five-membered rings have a symmetry higher than C_1. The ring strain energies for the four- and five-membered ring compounds (R = *i*Pr) were estimated on the basis of the homodesmotic reaction energies[28] [Equations (1) and (2)].

$$\begin{aligned}&Si^1R_2{-}X{-}SiR_2Si^3R_2(Si^1\text{-}Si^3) + 2\,SiHR_2{-}SiHR_2\\&+ 2\,SiHR_2{-}XH \rightarrow SiHR_2{-}X{-}SiHR_2\\&+ SiHR_2{-}SiR_2{-}SiHR_2 + 2\,SiHR_2{-}SiR_2{-}XH\end{aligned} \quad (1)$$

$$\begin{aligned}&Si^1R_2{-}X{-}SiR_2SiR_2{-}Si^4R_2(Si^1\text{-}Si^4) + 3\,SiHR_2{-}SiHR_2\\&+ 2\,SiHR_2{-}XH \rightarrow SiHR_2{-}X{-}SiHR_2\\&+ 2\,SiHR_2{-}SiR_2{-}SiHR_2 + 2\,SiHR_2{-}SiR_2{-}XH\end{aligned} \quad (2)$$

X-ray Crystal Analysis of 1−6: Crystals obtained from alcohols such as methanol, ethanol, and 2-propanol were used for X-ray analysis. Intensity data were obtained with an Enraf−Nonius CAD-4 diffractometer equipped with graphite-monochromated Cu-K_α (λ = 1.5418 Å) or Mo-K_α (λ = 0.7107 Å) radiation and by the ω-2θ scan technique. Structures of **1**−**6** were solved by direct methods with the MULTAN 78 program[39] and refined by full-matrix least squares. All the calculations were performed with the UNICS III system.[40] The molecular structures of **1b**, **2a**, **3a**−**d**,

Table 23. Crystal data, data collection, and refinement for five-membered silacycles $[R_2Si]_4X$ (X = NR^3)

	Compd		
	4a	**4b**	**4c**
		Crystal data	
formula	$C_{30}H_{67}NSi_4$	$C_{46}H_{99}NSi_4$	$C_{38}H_{83}NSi_4$
mol wt	554.208	778.637	666.422
crystal size/mm	0.4×0.3×0.2	0.4×0.4×0.4	0.36×0.36×0.13
cryst syst	Monoclinic	Orthorhombic	Monoclinic
space group	Pn	$P2_12_12_1$	$P2_1$
a/Å	10.550(1)	20.692(1)	11.157(1)
b/Å	10.964(1)	18.367(2)	16.375(1)
c/Å	15.551(1)	14.058(1)	13.068(2)
α/degree			
β/degree	97.70(1)		113.01(1)
γ/degree			
V/Å^3	1782.6(3)	5342.8(7)	2197.6(4)
Z	2	4	2
D_{calcd} (gcm^{-3})	1.032	0.9709	1.0072
		Data collection	
diffractmeter	Enraf-Nonius CAD4	Enraf-Nonius CAD4	Enraf-Nonius CAD4
radiation (λ/Å)	1.5418(CuKα)	1.5418(CuKα)	1.5418(CuKα)
temp/°C	23	23	23
scan mode	ω scan	ω scan	ω scan
scan range	4°∽120°	4°∽120°	4°∽120°
no. of reflns			
collected	2650	4413	3487
used (|Fo| ≧ 3σ | Fo|)	2532	3561	3227
μ/cm^{-1}	16.428	11.844	13.68
abs cor method	ψ scan	ψ scan	ψ scan
transmission factor (min/max)	0.9212/0.9998	0.8577/0.9991	0.9164/0.9994
		Solution and refinement	
system used	UNICS III	SDP-package and UNICS III	UNICS III
method	MULTAN 78	MULTAN 78	MULTAN 78
refinement method	full-matrix least squares	full-matrix least squares	full-matrix least squares
R (Rw)	0.058(0.071)	0.083(0.083)	0.052(0.073)
wrighting scheme	[a]	[b]	[c]
goodness of fit (S)	1.298	0.943	1.42
peaks in diff Fourier map (e/Å^3)	0.50/-0.50	0.7/-0.2	0.4/-0.4

[a] $w = 1/(0.047\cdot|F_o|^2 - 0.0280\cdot|F_o| + 0.4783)$. [b] $w = 1/(0.00295\cdot|F_o|^2 + 0.0781\cdot|F_o| + 1.929)$. [c] $w = 1/(0.0068\cdot|F_o|^2 - 0.118\cdot|F_o| + 1.113)$.

Table 24. Crystal data, data collection, and refinement for four- and five-membered silacycles $[R_2Si]nX$ (X = O)

	Compd		
	5b	**6a**	**6b**
	Crystal data		
formula	$C_{30}H_{66}OSi_3$	$C_{24}H_{56}OSi_4$	$C_{40}H_{88}OSi_4$
mol wt	527.107	473.048	697.477
crystal size/mm	0.2×0.2×0.2	0.4×0.3×0.2	0.3×0.2×0.1
cryst syst	Monoclinic	Monoclinic	Triclinic
space group	$P2_1$	$P2_1/n$	$\bar{P}1$
a/Å	11.250(2)	10.549(1)	20.742(2)
b/Å	16.015(1)	14.498(1)	21.454(1)
c/Å	11.715(4)	20.387(3)	11.431(1)
α/degree			97.06(1)
β/degree	119.28(2)	95.73(1)	100.96(1)
γ/degree			91.38(1)
V/Å^3	1841.3(9)	3102.1(5)	4950.2(5)
Z	2	4	4
D_{calcd} (gcm^{-3})	0.950	0.9355	0.936
	Data collection		
diffractmeter	Rigaku AFC-4	Enraf-Nonius CAD4	Rigaku RAXIS
radiation (λ/Å)	0.7107(MoKα)	1.5418(CuKα)	0.7107(MoKα)
temp/°C	23	23	15
scan mode	2θ/ω	ω scan	ω scan
scan range	4°∼55°	4°∼120°	4°∼55°
no. of refins			
collected	4438	4978	14760
used (|Fo| ≧ 3σ | Fo|)	1568	4208	4866
μ/cm^{-1}	1.47	17.86	1.44
abs cor method	no	ψ scan	no
transmission factor (min/max)	no	0.9367/0.9977	no
	Solution and refinrment		
system used	UNICS III	UNICS III	Texsan
method	MULTAN 78	MULTAN 78	SIR 92
refinement method	block diagonal least squares	full-matrix least squares	full-matrix least squares
R (Rw)	0.070(0.073)	0.074(0.083)	0.082(0.096)
wrighting scheme	[a]	[b]	[c]
goodness of fit (S)	2.33	1.959	2.38
peaks in diff Fourier map (e/Å^3)	0.42/-0.44	1.0/-0.64	0.40/-0.23

[a] $w = 1/\sigma^2 \cdot |F_o|$. [b] $w = 1/(0.00341 \cdot |F_o|^2 + 0.0961 \cdot |F_o| + 1.427)$. [c] $w = 1/\sigma^2 \cdot |F_o|$.

4a–**c**, **5b**, **6a**, and **6b** are given in the electronic supporting information. Selected bond lengths and bond and torsion angles are given in Tables 1–12, respectively. The crystallographic data for twelve four- and five-membered compounds are summarized in Tables 21–24. CCDC-169794 (**1b**), -169795 (**2a**), -169796 (**3a**), -169797 (**3b**), -169798 (**3c**), -169799 (**3d**), -169800 (**4a**), -169801 (**4b**), -169802 (**4c**), -169803 (**5b**), -169804 (**6a**), and -169805 (**6b**) contain the supplementary crystallographic data for this paper. These data can be obtained free of charge at www.ccdc.cam.ac.uk/conts/retrieving.html or from the Cambridge Crystallographic Data Centre, 12, Union Road, Cambridge CB2 1EZ, UK [Fax: (internat.) + 44-1223/336-033; E-mail: deposit@ccdc.cam.ac.uk].

Supporting Information: Supporting information for this article (Figures 6–17 with ORTEP drawings of molecular structures for **1**–**6**, and Figures 18–21 with UV spectral curves for **1**–**6**) is available (see also footnote on the first page of this article).

Acknowledgments

The authors are grateful to Toshiba Silicone Co., Ltd., and Shin-Etsu Chemical Co., Ltd., for a generous gift of chlorosilanes. The authors express their deep gratitude to the late Professor Yoichiro Nagai for helpful discussions at the early stage of this work, and also express thanks to Professors Hiroshi Hiratsuka and Shigefumi Tobita for helpful suggestions from the photochemical viewpoint. This work was partially supported (for H. W.) by Sansen Co., Ltd., Colcoat Co., Ltd., and the Gunma University Foundation for Promotion of Science and Technology.

[1] For reviews and references cited therein see: [1a] R. West, E. E. Carberry, *Science* **1975**, *189*, 179–186. [1b] H. Watanabe, Y. Nagai, in: *Organosilicon and Bioorganosilicon Chemisry* (Eds.: H. Sakurai), John Wiley & Sons, Inc., New York, **1985**, chapter 9, p. 105–114. [1c]T. Tsumuraya, A. Batcheller, S. Masamune, *Angew. Chem. Int. Ed. Engl.* **1991**, *30*, 902–930; *Angew. Chem.* **1991**, 103, 916. [1d] M. Weidenbruch, *Chem. Rev.* **1995**, *95*, 1479–1493. [1e] E. Hengge, R. Janoschek, *Chem. Rev.* **1995**, *95*, 1495–1526.

[2] [2a] A. Heine, D. Stalke, *Angew. Chem. Int. Ed. Engl.* **1994**, *33*, 113–115; *Angew. Chem.* **1994**, *106*, 121. [2b] E. Hengge, U. Brychy, *Monatsh. Chem.* **1966**, *97*, 1309–1317. [2c] E. Carberry, B. D. Dombek, *J. Organomet. Chem.* **1970**, *22*, C43–C47.

[3] [3a] G. Grunert, B. Fritz, *Z. Anorg. Allg. Chem.* **1981**, *473*, 59–79. [3b] M. Weidenbruch, J. Hamann, K. Peters, H. G. von Schnering, H. Marsmann, *J. Organomet. Chem.* **1992**, *441*, 185–195. [3c] M. Weidenbruch, J. Hamann, S. Pohl, W. Saak, *Chem. Ber.* **1992**, *125*, 1043–1046. [3d] D. Bravo-Zhivotovskii, Y. Apeloig, Y. Ovchinnikov, V. Igonin, Y. T. Struckov, *J. Organomet. Chem.* **1993**, *446*, 123–129. [3e] W. Ando, F. Hojo, S. Sekigawa, N. Nakayama, T. Shimizu, *Organometallics* **1992**, *11*, 1009–1011. [3f] M. Weidenbruch, E. Krobe, K. Peters, H. G. von Schnering, *J. Organomet. Chem.* **1993**, *461*, 35–38. [3g] S. A. Petrich, Y. Pang, G. Y. Young, Jr, T. J. Barton, *J. Am. Chem. Soc.* **1993**, *115*, 1591–1593. [3h] Y. Pang, S. A. Petrich, V. G. Young, Jr., M. S. Gordon, T. J. Barton, *J. Am. Chem. Soc.* **1993**, *115*, 2534–2536. [3i] H. Sanji, H. H. Hanao, H. Sakurai,

Chem. Lett. **1997**, 1121−1122. [3j] R. Imhof, H. Teramae, J. Michl, *Chem. Phys. Lett.* **1997**, *270*, 500−505. [3k] For Si_2C cycles, see ref.[1d]

[4] For Si_2N and Si_4N cycles, see refs.[1d,2b]

[5] [5a] H. Watanabe, T. Muraoka, M. Kageyama, Y. Nagai, *J. Organomet. Chem.* **1981**, *216*, C45−C47. [5b] S. Masamune, H. Tobita, S. Murakami, *J. Am. Chem. Soc.* **1983**, *105*, 6524−6525. [5c] M. Weidenbruch, A. Schaefer, *J. Organomet. Chem.* **1984**, *209*, 231−234. [5d] C. W. Carlson, R. West, *Organometallics.* **1983**, *2*, 1801−1807. [5e] B. J. Helmer, R. West, *Organometallics* **1982**, *1*, 1463−1466. [5f] L. Parkanyi, E. Hengge, H. Stuger, *J. Organomet. Chem.* **1983**, *251*, 167−174. [5g] S. Willms, A. Grybat, W. Saak, M. Weidenbruch, *Z. Anorg. Allg. Chem.* **2000**, *626*, 1148−1152. [5h] For Si_2O cycles, see ref.[1d] and references cited therein.

[6] [6a] Calculated geometries of $[H_2Si]_nX$ (n = 2, 3; X = SiH_2, CH_2, O, S, PH, NH): S. R. Grev, H. F. Schaefer III, *J. Am. Chem. Soc.* **1987**, *109*, 6577−6585. [6b] UV spectra of $[Me_2Si]_nX$ (n = 4−6; X = NMe, PMe): R. West, *Pure Appl. Chem.* **1982**, *54*, 1041−1050. [6c] UV spectra of $[Me_2Si]_nX$ (n = 4−6; X = NMe, PMe): T. H. Newman, R. West, R. F. Oakley, *J. Organomet. Chem.* **1980**, *197*, 159−168. [6d] UV and NMR spectra of $[Me_2Si]_nX$ (n = 4−6; X = O, S, Se, NMe, PMe): H. Stuger, M. Eibl, E. Hengge, *J. Organomet. Chem.* **1992**, *431*, 1−15. [6e] UV spectra of $[Ph_2Si]_{4-}X$ (X = $BNMe_2$, O, NMe, NEt): E. Hengge, D. Wolfer, *J. Organomet. Chem.* **1974**, *66*, 413−424.

[7] [7a] H. Watanabe, M. Kato, T. Okawa, Y. Nagai, M. Goto, *J. Organomet. Chem.* **1984**, *271*, 225−233. [7b] H. Watanabe, T. Okawa, M. Kato, Y. Nagai, *J. Chem. Soc., Chem. Commun.* **1983**, 781−782. [7c] H. Watanabe, Y. Kougo, Y. Nagai, *J. Chem. Soc., Chem. Commun.* **1984**, 66−67. [7d] H. Watanabe, T. Muraoka, M. Kageyama, M. Yoshizumi, Y. Nagai, *Organometallics* **1984**, *3*, 141−147. [7e] H. Watanabe, H. Shimoyama, T. Muraoka, T. Okawa, M. Kato, Y. Nagai, *Chem. Lett.* **1986**, 1057−1058. [7f] H. Watanabe, M. Kato, O. Okawa, Y. Kougo, Y. Nagai, M. Goto, *Appl. Organomet. Chem.* **1987**, *1*, 157−169. [7g] H. Watanabe, Y. Kougo, M. Kato, H. Kuwabara, H. Okawa, Y. Nagai, *Bull. Chem. Soc. Jpn.* **1984**, *57*, 3019−3020. [7h] H. Watanabe, K. Yoshizumi, M. Kato, T. Muraoka, Y. Nagai, T. Sato, *Chem. Lett.* **1985**, 1683−1686.

[8] H. Watanabe, E. Tabei, M. Goto, Y. Nagai, *Chem. Commun.* **1987**, 522−523.

[9] H. Suzuki, K. Okabe, S. Uchida, H. Watanabe, M. Goto, *J. Organomet. Chem.* **1996**, *509*, 177−188.

[10] H. Suzuki, K. Okabe, R. Kato, N. Sato, Y. Fukuda, H. Watanabe, M. Goto, *Organometallics* **1993**, *12*, 4833−4842.

[11] H. Suzuki, K. Tanaka, B. Yoshizoe, T. Yamamoto, N. Kenmotsu, S. Matuura, T. Akabane, H. Watanabe, M. Goto, *Organometallics* **1998**, *17*, 5091−5101.

[12] [12a] J. J. P. Stewart, *J. Comput. Chem.* **1989**, *10*, 209−220. [12b] J. J. P. Stewart, *J. Comput. Chem.* **1989**, *10*, 221−264.

[13] W. S. Sheldrick, in: *The Chemistry of Organic Silicon Compounds* (Eds.: S. Patai, Z. Rappoport), John Wiley & Sons, Inc., New York, **1989**, chapter 3, pp. 227−303 and references cited therein.

[14] R. Tanaka, M. Unno, H. Matsumoto, *Chem. Lett.* **1999**, 595−596.

[15] M. J. Michalczyk, M. J. Fink, K. J. Haller, R. West, M. Michl, *Organometallics* **1986**, *5*, 531−538.

[16] H. Matsumoto, M. Minemura, K. Takatsuna, Y. Nagai, M. Goto, *Chem. Lett.* **1985**, 1005−1006.

[17] R. W. Taft, Jr., in: *Steric Effects in Organic Chemistry* (Ed.: M. S. Newman), John Wiley & Sons, Inc., Tokyo Maruzen Co. Ltd., **1956**, chapter 13, pp. 559−675.

[18] [18a] A. T. Gordon, R. A. Ford (Eds.), *The Chemist's Companion, A Handbook of Practical Data, Techniques, and References*, John Wiley & Sons, Inc., New York, **1972**, pp. 82−87 and references cited therein; A. L. Allred, E. G. Rochow, *J. Inorg. Nucl. Chem.* **1958**, *5*, 264−268, 269−288. [18b] A. L. Allred, *J. Inorg. Nucl. Chem.* **1961**, *17*, 215−221.

[19] C. Liang, L. C. Allen, *J. Am. Chem. Soc.* **1991**, *113*, 1878−1884.

[20] E. A. Williams, in: *The Chemistry of Organic Silicon Compounds* (Eds.: S. Patai, Z. Rappoport), John Wiley & Sons, Inc., New York, **1989**, chapter 8, pp. 511−554 and references cited therein.

[21] R. K. Harris, B. J. Kimber, *Adv. Mol. Relax. Processes* **1976**, *8*, 23−35.

[22] [22a] M. Biernbaum, R. West, *J. Organomet. Chem.* **1977**, *131*, 179−188. [22b] E. Carberry, R. West, G. E. Gross, *J. Am. Chem. Soc.* **1969**, *91*, 5446−5451. [22c] C. W. Carlson, R. West, *Organometallics* **1983**, *2*, 1792−1797.

[23] H. Gilman, W. H. Atwell, G. L. Schwebke, *J. Organomet. Chem.* **1964**, *2*, 369−371.

[24] [24a] A. F. Sax, *Chem. Phys. Lett.* **1986**, *127*, 163−168. [24b] S. Nagase, M. Nakano, T. Kudo, *J. Chem. Soc., Chem. Commun.* **1987**, 60−62. [24c] R. S. Grev, H. F. Schaefer III, *J. Am. Chem. Soc.* **1987**, *109*, 6569−6585. [24d] D. B. Kitchen, J. E. Jackson, L. C. Allen, *J. Am. Chem. Soc.* **1990**, *112*, 3408−3414. [24e] M. Zhan, B. M. Gimarc, *Inorg. Chem.* **1996**, *35*, 5378−5386.

[25] M.-C. Ou, S.-Y. Chu, *J. Mol. Struct. (Theochem).* **1995**, *357*, 141−146.

[26] [26a] S. Inagaki, K. Yoshikawa, Y. Hayano, *J. Am. Chem. Soc.* **1993**, *115*, 3706−3709. [26b] S. Inagaki, Y. Ishitani, T. Kakefu, *J. Am. Chem. Soc.* **1994**, *116*, 5954−5958.

[27] Preparations for advanced calculations are currently underway.

[28] [28a] P. George, M. Trachtman, C. W. Bock, A. M. Brett, *Tetrahedron* **1976**, *32*, 317−323. [28b] P. George, M. Trachtman, C. W. Bock, A. M. Brett, *J. Chem. Soc., Perkin Trans. 2* **1976**, 1222−1227. [28c] P. George, M. Trachtman, A. M. Brett, C. W. Bock, *J. Chem. Soc., Perkin Trans. 2* **1997**, 1036−1047.

[29] F. Shafiee, R. West, *Silicon, Germanium, Tin Lead Compd.* **1986**, *9*, 1−10.

[30] For organometallic compounds: [30a] H. C. Gardner, J. K. Kochi, *J. Am. Chem. Soc.* **1975**, *97*, 1855−1865. [30b] R. J. Klingler, J. K. Kochi, *J. Am. Chem. Soc.* **1980**, *102*, 4790−4798. [30c] K. Mochida, A. Itani, M. Yokoyama, T. Tsuchiya, S. D. Worley, J. K. Kochi, *Bull. Chem. Soc. Jpn.* **1985**, *58*, 2149−2150. [30d] H. Bock, U. Lechner-Knoblauch, *J. Organomet. Chem.* **1985**, *294*, 295−304.

[31] [31a] T. Takami, S. Masuda, K. Ohno, Y. Harada, Y. Yagihashi, H. Matsumoto, Y. Nagai, *The 56th National Meeting of the Japan Chemical Society*, Tokyo, **1988**, Abstracts 1IVB27, p. 513. [31b] Y. Yagihashi, Master Thesis, The Graduate School of Engineering, Gunma University, March **1988**.

[32] T. F. Block, M. Biernbaum, R. West, *J. Organomet. Chem.* **1977**, *131*, 199−205.

[33] T. F. Block, M. Biernbaum, R. West, *J. Organomet. Chem.* **1974**, *77*, C13−C14.

[34] H. Shizuka, K. Murata, Y. Arai, K. Tonokura, H. Tanaka, H. Matsumoto, Y. Nagai, G. Gillette, R. West, *J. Chem. Soc., Faraday Trans. 1* **1989**, *85*, 2369−2377.

[35] H. Bock, W. Ensslin, *Angew. Chem.* **1971**, *83*, 435−437; *Angew. Chem. Int. Ed. Engl.* **1971**, *10*, 404−405.

[36] N. J. Turro, *Modern Molecular Photochemistry*, The Benjamain/Cummings Publishing Co., Inc., Menlo Park, California, **1978**, pp. 103−117.

[37] Unpublished work: [37a] H. Watanabe, E. Tabei, N. Hirai, M. Yoshikawa, H. Ohmori, M. Nishiyama, M. Sugo, S. Takahashi, K. Ohyama: Photochemical decompositions of $(R_2Si)_nX$ (R = *i*Pr, *t*$BuCH_2$; n = 3, 4; X = C, N, O; see ref.[8]). [37b] H. Watanabe, T. Adachi: Photosensitized decompositions of $(R_2Si)_nX$ (R = *i*Pr, *t*$BuCH_2$; n = 3, 4; X = C, N, O) by electrontransfer.

[38] H. Watanabe, H. Shimoyama, T. Muraoka, Y. Kougo, Y. Kato, Y. Nagai, *Bull. Chem. Soc. Jpn.* **1987**, *60*, 769−770.

[39] P. Main, S. E. Hull, L. Lessinger, G. Germain, J. Declercq, M. M. Woolfson, *MULTAN 78, A System of Computer Programs for the Automatic Solution of Crystal Structures for the X-ray Diffraction Data*, University of York, England, and Louvain, Belgium, **1978**.

[40] T. Sakurai, K. Kobayashi, *Rikagakukenkyujyo Houkoku* **1979**, *55*, 69−77.
[41] H. Watanabe, M. Aoki, H. Matsumoto, Y. Nagai, *Bull. Chem. Soc. Jpn.* **1977**, *50*, 1019−1020.
[42] M. J. Frish, G. W. Trucks, H. B. Schlegel, G. E. Scuseria, M. A. Robb, J. R. Cheeseman, V. G. Zakrzewski, J. A. Montogomery, R. E. Stratmann, J. C. Burant, S. Dapprich, J. M. Millam, A. D. Daniels, K. N. Kudin, M. C. Strain, O. Farkas, J. Tomasi, V. Barone, M. Cossi, R. Cammi, B. Mennuecci, C. Ponmelli, C. Adamo, S. Clifford, J. Ochterski, G. A. Petersson, P. Y. Ayala, Q. Cui, K. Morokuma, D. K. Malick, A. D. Rabuck, K. Raghavachari, J. B. Foresman, J. Cioslowski, J. V. Ortiz, B. B. Stefanov, G. Liu, A. Liashenko, P. Piskorz, I. Komaromi, D. J. Fox, R. L. Martin, R. Gomperts, T. Keith, M. A. Al-Laham, A. Nanayakkara, C. Y. Peng, A. Nanayakkara, C. Gonzalez, M. Challacombe, P. M. W. Cill, B. G.Jonson, W. Chen, M. W. Wong, J. L. Andres, M. Head-Gordon, E. S. Replogle, J. A. Pople, *GAUSSIAN98*, Gaussian, Inc., Pittsburgh, PA, **1998**.
[43] M. W. Schmidt, K. K. Baldridge, J. A. Boatz, S. T. Elbert, M. S. Gordon, J. H. Jensen, S. Koseki, N. Matsunaga, K. A. Nguyen, S. Su, T. L. Windus, M. Dupuis, J. A. Montgomery, Jr., *J. Comput. Chem.* **1993**, *14*, 1347−1363.

Received September 10, 2001
[I01354]